

# **Universitätsklinikum Hamburg-Eppendorf**

Zentrum für Molekulare Neurobiologie Hamburg

Institut für Synaptische Physiologie

Prof. Dr. Thomas Oertner

**The Role of the TRPM4 channel in fundamental properties of microglia**

## **Dissertation**

zur Erlangung des Grades eines Doktors der Medizin  
an der Medizinischen Fakultät der Universität Hamburg.

vorgelegt von:

Ana Margarida Cavaco Antunes

aus Lissabon, Portugal

Hamburg 2022

**Angenommen von der  
Medizinischen Fakultät der Universität Hamburg am:**

**Veröffentlicht mit Genehmigung der  
Medizinischen Fakultät der Universität Hamburg.**

**Prüfungsausschuss, der/die Vorsitzende: Prof. Dr. Manuel Friese**

**Prüfungsausschuss, zweite/r Gutachter/in: Prof. Dr. Thomas Oertner**

**Mündliche Prüfung am 17. April 2023**

*”À dolorosa luz das grandes lâmpadas eléctricas da fábrica*

*Tenho febre e escrevo.*

*Escrevo rangendo os dentes, fera para a beleza disto,*

*Para a beleza disto totalmente desconhecida dos antigos.”*

*Álvaro de Campos*

# Contents

<b>List of Figures</b>	<b>v</b>
<b>Background and Work hypothesis</b>	<b>vi</b>
<b>1 Introduction</b>	<b>1</b>
<b>1.1 Multiple sclerosis and Experimental autoimmune encephalomyelitis .</b>	<b>1</b>
<b>1.2 Microglia . . . . .</b>	<b>3</b>
<b>1.3 TRPM4 . . . . .</b>	<b>6</b>
<b>2 Materials and Methods</b>	<b>13</b>
<b>2.1 Animals and slice culture . . . . .</b>	<b>13</b>
<b>2.1.1 Mice . . . . .</b>	<b>13</b>
<b>2.1.2 Mouse Genotyping . . . . .</b>	<b>13</b>
<b>2.1.3 Mouse organotypic slice cultures . . . . .</b>	<b>14</b>
<b>2.2 Two-photon microscopy . . . . .</b>	<b>15</b>
<b>2.2.1 Motility and chemotaxis (laser damage) experiments . . . . .</b>	<b>16</b>
<b>2.2.2 Image analysis . . . . .</b>	<b>16</b>
<b>2.3 Immunohistochemistry . . . . .</b>	<b>18</b>
<b>2.3.1 Perfusion of animals, treatment of cultures and slice fixation .</b>	<b>18</b>
<b>2.3.2 Staining . . . . .</b>	<b>18</b>
<b>2.3.3 Confocal microscopy . . . . .</b>	<b>19</b>
<b>2.4 Statistics . . . . .</b>	<b>20</b>
<b>3 Results</b>	<b>23</b>
<b>3.1 Microglia motility is not affected by acute block of TRPM4 . . . . .</b>	<b>23</b>

3.2	Microglia surveillance is not affected by long-term block or KO of TRPM4 . . . . .	25
3.3	LPS-induced inflammation decreases ramification of WT and TRPM4 lacking microglia . . . . .	27
3.4	KO microglia are also more ramified <i>ex vivo</i> . . . . .	27
3.5	TRPM4 KO microglia respond slower to laser damage than WT ones	30
4	Discussion	34
4.1	TRPM4 and the motility of microglia . . . . .	34
4.2	TRPM4 and the morphology of microglia . . . . .	35
4.3	TRPM4 and the laser damage response of microglia . . . . .	36
4.4	TRPM4 and temperature . . . . .	37
4.5	General considerations and perspectives . . . . .	37
5	Abstract/Zusammenfassung	39
6	List of abbreviations	40
	Bibliography	42
7	Acknowledgements	49
8	Curriculum Vitae	51
9	Eidesstattliche Versicherung	52

# List of Figures

<b>1.1</b>	<b>Pathophysiology of MS</b>	<b>3</b>
<b>1.2</b>	<b>Microglia and its functions in maintaining the status quo in the CNS</b>	<b>4</b>
<b>1.3</b>	<b>Schematic overview of microglial roles in MS</b>	<b>6</b>
<b>1.4</b>	<b>TRP channel family tree</b>	<b>7</b>
<b>1.5</b>	<b>TRPM4 channel and its modulating molecules</b>	<b>8</b>
<b>1.6</b>	<b>Chemical structures of TRPM4 inhibitors</b>	<b>10</b>
<b>1.7</b>	<b>TRPM4 in EAE</b>	<b>11</b>
<b>2.1</b>	<b>Morphology experiment</b>	<b>21</b>
<b>2.2</b>	<b>Image analysis of microglial motility</b>	<b>22</b>
<b>2.3</b>	<b>Spot detection</b>	<b>22</b>
<b>3.1</b>	<b>Microglia motility is not affected by acute block of TRPM4</b>	<b>24</b>
<b>3.2</b>	<b>Baseline motility of microglia at 32°C and 36°C</b>	<b>26</b>
<b>3.3</b>	<b>TRPM4 KO microglia are more ramified than WT microglia</b>	<b>28</b>
<b>3.4</b>	<b>Morphology of TRPM4 KO microglia <i>ex vivo</i></b>	<b>29</b>
<b>3.5</b>	<b>Inhibition of TRPM4 decreases the response of microglia to laser damage.</b>	<b>32</b>
<b>3.6</b>	<b>Knock out of TRPM4 decreases the responses of microglia to laser damage.</b>	<b>33</b>

# Background and Work hypothesis

## **The Role of the TRPM4 channel in fundamental properties of microglia**

Microglia are the only resident immune cells in the central nervous system (CNS) and stimulate both pro- and anti-inflammatory responses. In the past years microglia have been shown to play an important role in maintaining homeostasis in the CNS, while at the same time being key players in the development of neurodegenerative diseases like Alzheimer's disease or Multiple Sclerosis (MS). The mechanisms that contribute to the axonal and neuronal damage characteristic of these diseases are unknown.

In a recently published study (Schattling et al. 2012), the ion channel Transient Receptor Potential Melastatin 4 (TRPM4) was shown to have a negative influence in the disease course of a MS mouse model. The pharmacological inhibition or genetic knock-out of TRPM4 induced neuroprotective effects, drastically improving clinical score in mice with Experimental Autoimmune Encephalomyelitis (EAE). These effects were attributed to a reduced vulnerability for excitotoxicity caused by TRPM4 knock-out in neurons. Potential protective mechanisms involving microglial TRPM4 have not yet been investigated and could play an important role in this neuroprotective effect of TRPM4 block.

The goal of this study was to investigate the role of TRPM4 activation in microglia, which potentially contributes to the inflammatory processes and disease course of MS.

# Chapter 1

## Introduction

### 1.1 Multiple sclerosis and Experimental autoimmune encephalomyelitis

Multiple sclerosis (MS) is a chronic inflammatory, neurodegenerative and demyelinating disease. It is established to be the most prevalent cause of neurological disability in young adults. Among the few currently available therapy options, no curative treatment is available. The use of immunomodulators is helpful in reducing relapse frequency but tools are lacking to actually stop the disease progression (Compston and Coles 2008). MS is a polysymptomatic disease. Patients often show impairment in multiple functions to different degrees, such as mobility, hand function, vision, fatigue, cognition, bowel and bladder function, sensation, spasticity, pain, depression, tremor/coordination (McDonald and Compston 2006, Kister et al. 2013). There are four clinical MS subtypes: relapsing-remitting (RR), secondary-progressive (SP), primary-progressive (PP) and progressive-relapsing (PR) (Lublin et al. 2014).

The causes of MS are unknown and most likely multifactorial. Environmental exposure (overweight, smoking, lack of vitamin D) and genetic predisposition (family history, some genes of the human leucocyte antigen (HLA) system) serve as risk factors for the disease (Compston and Coles 2008). The pathogenesis begins with a central nervous system (CNS) inflammatory cascade, predominantly caused by T-cells and also by B-cells that disrupt the blood-brain-barrier (BBB) and manage to cross it. They drive local in-



## CHAPTER 1. INTRODUCTION

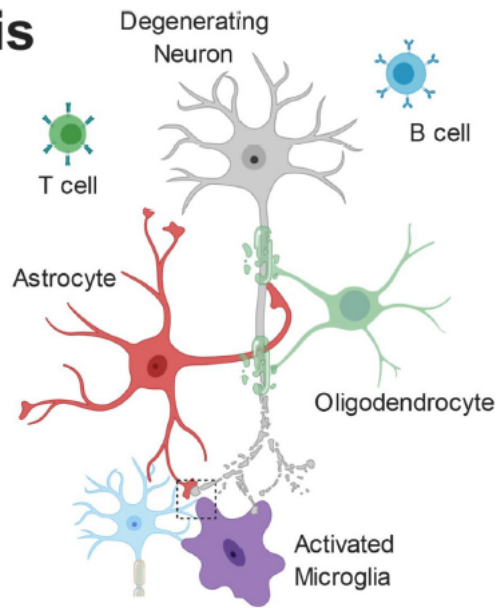
flammatory responses against myelin and myelin-making oligodendrocytes, resulting in lesions (Dendrou, Fugger, and Friese 2015). So far the state of knowledge involves different processes and mechanisms leading to disease progression, such as chronic demyelination, gliosis, axonal loss and unbalanced damage and repair. Also one major mechanism can be the interaction between CNS-infiltrating lymphocytes and CNS-resident cells, the microglia (Lucchinetti et al. 2011). Indeed, neuropathological studies have shown the presence of demyelination and axonal damage in gray matter of MS patients, in association with microglial activation, while lymphocytes are located in the meninges (Magliozzi et al. 2007). However, the mechanisms that lead to significant neuronal damage and axonal injury under inflammatory conditions are still not very well understood and further investigation is needed in this field (Figure 1.1).

There are several animal models already established to study MS. It is very difficult to experimentally test the role of a specific molecule or gene by studying patients, so animal models for the study of the disease are optimal. The most widely used is without question the experimental autoimmune encephalomyelitis (EAE) of the mouse and as such has been a powerful tool for studying disease pathogenesis as well as potential therapeutic interventions (Glatigny and Bettelli 2018). It consists of a T-helper (Th) cell-mediated autoimmune disease characterized by T-cell and monocyte infiltration in the CNS associated with local inflammation. Mostly utilized as molecular targets are proteins expressed by myelin-producing oligodendrocytes in the CNS (A. P. Robinson et al. 2014). A protein that is commonly used for immunization is the myelin oligodendrocyte glycoprotein (MOG) (Amor et al. 1994). Typically, between 7–12 days after immunization, infiltrating inflammatory cells attack the myelin sheath, resulting in primary demyelination of axonal tracks, impaired axonal conduction in the CNS, leading to motor deficits and ascending paralytic disease. These defects are quantified using a standard EAE scoring system on a 0 – 5 disease severity scale, based on the animals motility and behaviour: 0, no disease; 1, loss of tail tone; 2, hind limb weakness; 3, hind limb paralysis; 4, hind limb paralysis and forelimb paralysis or weakness; and 5, moribund/death (Shahi et al. 2019). The animal protection law allows for experiments on mice until the degree 3 is reached.

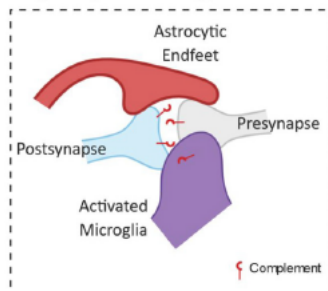
# Multiple Sclerosis

## Pathological Changes

- Loss of **myelin sheath**
- **Autoimmune** response (T and B cell activation)
- Gliosis
- Release of pro-inflammatory mediators - **neuroinflammation**
- Disrupted synaptic glutamate handling - **excitotoxicity**



## Synapse Engulfment



## Current Knowledge

- Complement tagging of synapses
- Little evidence of microglia phagocytosing pre-synapses
- Robust human data is lacking

**Figure 1.1: Pathophysiology of MS.** While myelin loss is a central feature of MS pathology, it is accompanied by neurodegeneration, gliosis and immune cell (B-cells and T-cells) infiltration. Release of pro-inflammatory mediators and disrupted glutamate handling by glial cells leads to a toxic neuronal milieu. Furthermore, there is evidence that microglia are involved in complement-dependent synapse engulfment. Figure from Henstridge, Tzioras, and Paolicelli 2019.

## 1.2 Microglia

Microglia are the primary immune cells of the brain (Perry and Gordon 1988). Originally they develop from the immature yolk sac precursor cells during early embryogenesis, migrating to the brain and persisting throughout life (Ginhoux et al. 2013). They are busy and vigilant housekeepers of their environment, responding to internal or external brain damage by becoming activated and undergoing functional and structural changes.

## CHAPTER 1. INTRODUCTION

They are about 5 to 15% of all brain cells. In a resting state, they are highly ramified around a small, central soma and spread over about 50  $\mu\text{m}$  in diameter (Nimmerjahn, Kirchhoff, and Helmchen 2005) (Figure 1.2). Microglia are deeply involved in all phases of the MS disease process (Jack et al. 2005) and can have a variety of roles. They produce pro-inflammatory cytokines and reactive oxygen species (ROS), thereby causing neurodegeneration and axonal damage (O’Loughlin et al. 2018). In addition to the focal lesions, activated microglia are found in the normal-appearing white matter (NAWM) of MS patients, the area surrounding the focal lesion (Poel et al. 2019). When microglia become activated, their morphology changes, characterized by retraction of their processes around an enlarged soma. The degree of activation also increases with the progression of the disease, while in disease inactivity its restoration was observed (Zrzavy et al. 2017).

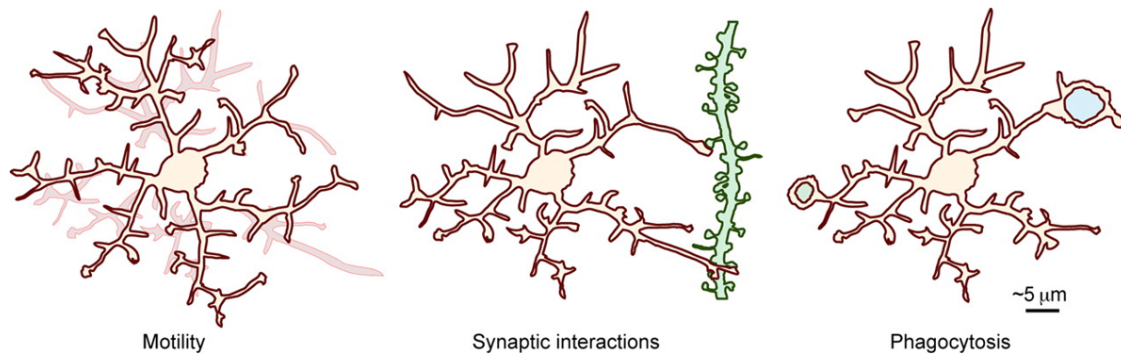


**Figure 1.2: Microglia and its functions in maintaining the status quo in the CNS.** Microglial processes extend and retract around the surrounding environment (motility). Microglia can also interact with neurons and phagocyte particles. Figure from Trepel 2017.

Activation of microglia is driven by soluble factors produced by T and B cells that enter the CNS, while at the same time the activated microglia and astrocytes can contribute to the persistence of these cells within the CNS by means of secretion of pro-inflammatory factors such as interleukin (IL) - 6 and B-cell activating factor (BAFF) (Krumbholz et al. 2005). On the other hand, microglia can also have neuroprotective functions. Very importantly, they undergo myelin debris clearance by phagocytosis to induce remyelination and therefore contribute to neuronal repair, at the same they are able to produce anti-inflammatory cytokines (Lampron et al. 2015). So it would be interest-

## CHAPTER 1. INTRODUCTION

ing for therapy to promote a transition of microglia from a pro-inflammatory phenotype to an anti-inflammatory one, since the anti-inflammatory microglia support the remyelination by having a key role in sterol synthesis (Berghoff et al. 2021). However the exact mechanism remains unknown, one possible being microglia death. A recent study showed that necroptosis of microglia is important in the phenotype transition during remyelination. The authors suggest that microglia may not switch between phenotypes, but pro-inflammatory microglia are dying in order to be replaced by anti-inflammatory ones (Lloyd et al. 2019).

Given the different roles of microglia in regulating the pathology of MS, a balance between limiting demyelination and boosting remyelination might be a valuable strategy for patients with a progressive disease course. Microglia are indeed very versatile because of the fact that they can have both neuroprotective and neurotoxic effects when they become activated (Geladaris, Häusler, and M. S. Weber 2021) (Figure 1.3). Overall this effect may depend on both pathologic conditions and injury severity (Rossum and Hanisch 2004, Raivich et al. 1999).

Microglia are very motile cells in the resting state and when they become activated too. Microglia motility most likely has its basis in actin, a cytoskeletal protein shown to be critically involved in growth and motility in many cells. Indeed, microglia contain high amounts of filamentous actin (Capani, Ellisman, and Martone 2001), and inhibitors of actin polymerization have been shown to affect the motility and migration of activated microglial cells (Nolte et al. 1996). It would be interesting to investigate what factors exactly could take a part in modulating this process. A study published this year showed that mouse microglia exhibit temperature-dependent motility/movement *in vitro* and *in vivo* that is mediated by some members of the transient receptor potential (TRP) channel family (Nishimoto et al. 2021).

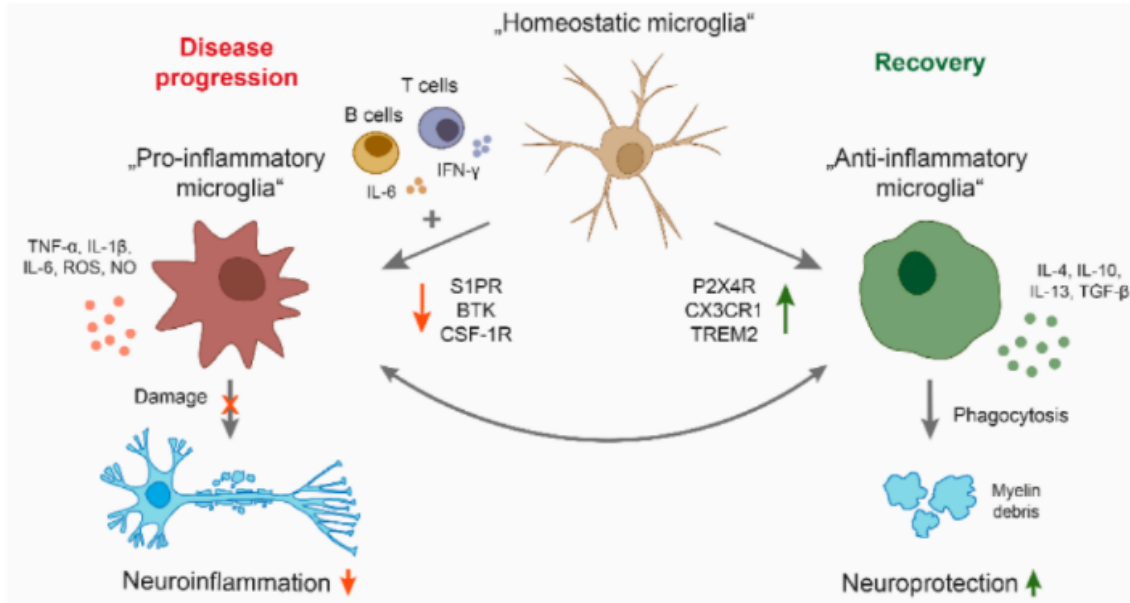


**Figure 1.3: Schematic overview of microglial roles in MS.** During disease progression, a CNS compartmentalized milieu generated by pro-inflammatory B and T cells leads to a reactive phenotype of microglia with neuroinflammatory properties. By secreting cytokines and upregulation of particular cell surface molecules, the activated microglia trigger oligodendrocyte damage, resulting in demyelination, axonal damage, and neuronal loss. Microglia also have important physiological functions in maintaining tissue homeostasis, including clearance of debris, resulting in neuroprotection. Candidate drugs for treatment of MS progression may act on following therapeutic principles: either inhibiting pro-inflammatory (Sphingosine-1-phosphate (S1P), Bruton’s tyrosine kinase (BTK), Colony-stimulating factor 1 receptor (CSF-1R)) or enhancing anti-inflammatory properties of microglia (Purinergic receptor P2X4 (P2X4R), CX3 chemokine receptor 1 (CX3CR1), Triggering receptor expressed on myeloid cells 2 (TREM2)). Figure from Geladaris, Häusler, and M. S. Weber 2021.

### 1.3 TRPM4

The Transient Receptor Potential (TRP) channels are a big family of 28 members widely expressed in a range of tissues and different cell types. The majority of these cation channels are permeable to both monovalent and divalent cations and they can be subdivided into six subgroups: TRPC (canonical), TRPV (vanilloid), TRPM (melastatin), TRPP (polycystin), TRPML (mucolipin) and TRPA (ankyrin) (Gees, Colsoul, and Nilius

2010) (Figure 1.4).

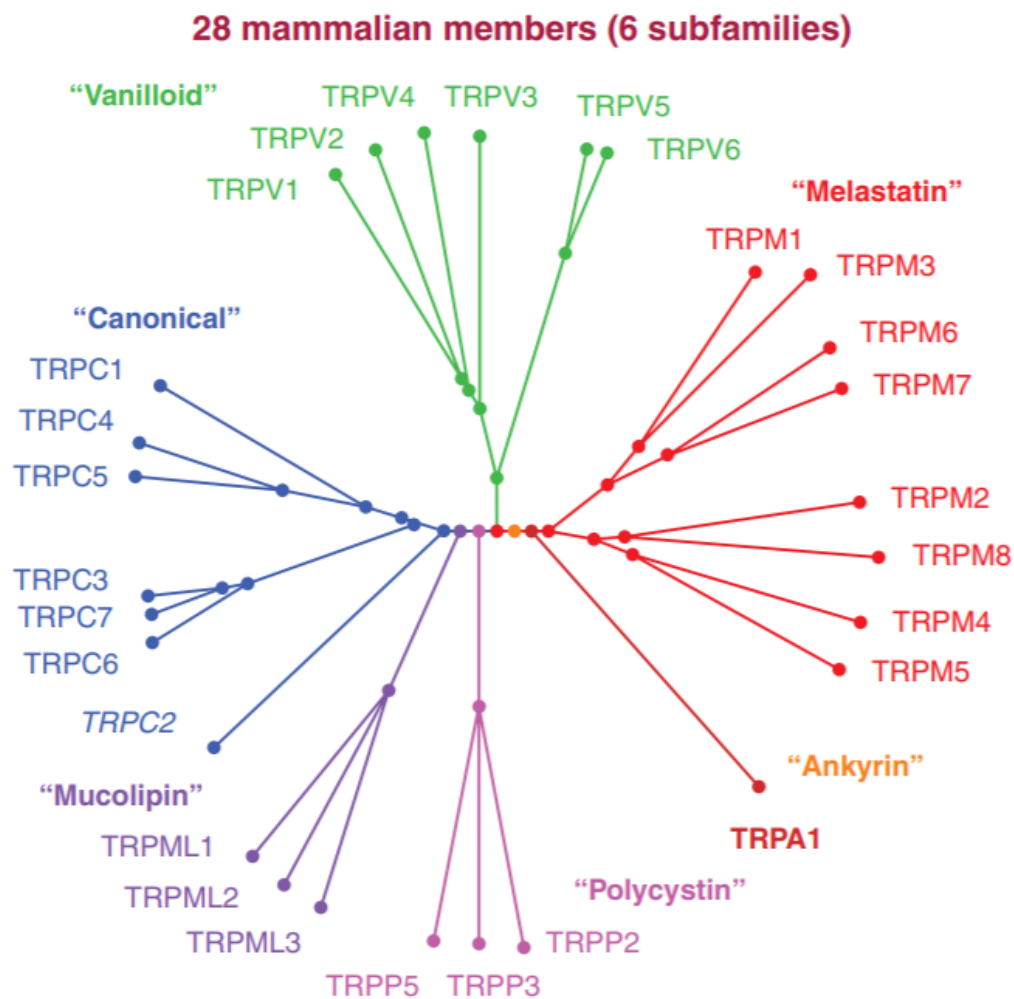


**Figure 1.4: TRP channel family tree.** Figure from Gees, Colsoul, and Nilius 2010.

Transient receptor potential melastatin 4 (TRPM4), a member of the melastatin branch of the TRP channels, is a monovalent selective cation channel that is activated by cytoplasmic  $\text{Ca}^{2+}$  (Launay, Fleig, et al. 2002). TRPM4’s closest relative is TRPM5, which also forms a  $\text{Ca}^{2+}$  - activated cation channel. Its expression is, however, less ubiquitous than that of TRPM4, being predominantly in the taste receptor cells, olfactory neurons and other chemosensory tissues (Liman 2014) and is correspondingly involved in some forms of sensory transduction (Y. Zhang et al. 2003). Although the TRPM4 channel is impermeable to  $\text{Ca}^{2+}$ , it plays a role in the modulation of intracellular  $\text{Ca}^{2+}$ . The depolarization induced by TRPM4 decreases  $\text{Ca}^{2+}$  entry by decreasing the driving force (Gees, Colsoul,

and Nilius 2010). The TRPM4 channel has been reported to be inhibited by intracellular adenosine triphosphate (ATP) in some conditions (Nilius et al. 2005). Phosphatidylinositol 4,5-bisphosphate (PIP2) can rescue the channel's desensitization (Z. Zhang et al. 2005) and calmodulin binding as well as protein kinase C (PKC) phosphorylation have been shown to increase the channel's sensitivity to  $\text{Ca}^{2+}$  (Nilius et al. 2005). The opening of the TRPM4 channel is also known to have temperature sensitivity, similarly to TRPM5 (Talavera et al. 2005) and many other TRP channels (Nishimoto et al. 2021) (Figure 1.5).

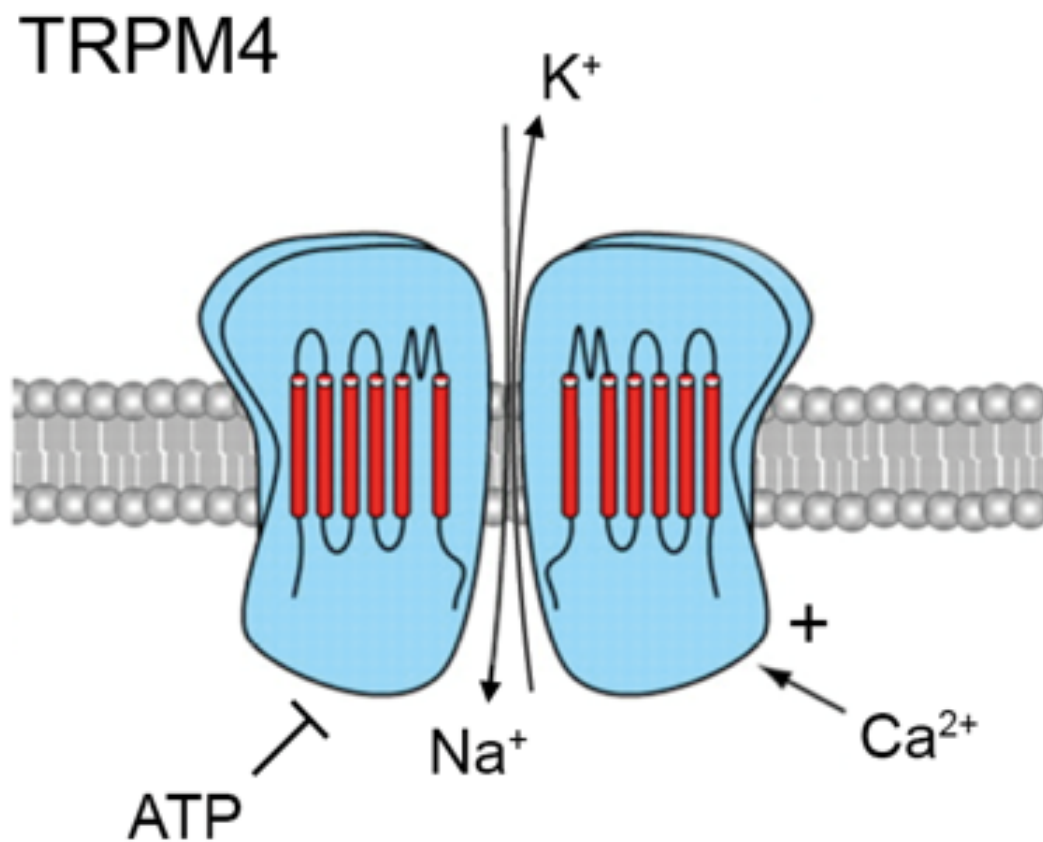


**Figure 1.5: TRPM4 channel and its modulating molecules.** The TRPM4 is a monovalent selective cation channel inhibited by intracellular ATP and is sensitive to intracellular  $\text{Ca}^{2+}$ , being at the same time impermeable to it. Figure from Dr. Jan Broder Engler.

A lack of potent specific antagonists is a challenge for studying TRPM4. Some pharmacological agents have been already described (Figure 1.6). 9-Phenanthrol is a compound that has been known for a long time (Moriconi, Wallenberger, and O'Connor 1959). In a 2008 study it was shown to be a specific antagonist of TRPM4 and not of TRPM5

## CHAPTER 1. INTRODUCTION

(Grand et al. 2008). In spite of this, it has a number of off-target effects, to name one also the antagonism of Transmembrane member 16A (TMEM16A), a  $\text{Ca}^{2+}$  - activated chloride channel (Burriss et al. 2015). A very commonly used anti-diabetic drug Glibenclamide also acts as a TRPM4 antagonist. It is a sulfonylurea that targets the K - ATP channels in the pancreatic islet beta-cells responsible for insulin secretion (Ashcroft et al. 2005). These channels have as a subunit a sulfonylurea receptor 1 (SUR1), that acts as an ion channel regulator (Aittoniemi et al. 2009) and has been shown to form a heteromeric channel with TRPM4 (Woo et al. 2013). SUR1 - TRPM4 channels are rare under normal conditions, but are newly upregulated in a variety of CNS disorders (Simard et al. 2012). In a 2018 study, another compound was shown to be highly selective for TRPM4, its name 4-chloro-2-[[2-(2-chlorophenoxy)acetyl]amino]benzoic acid (CBA), originally published as compound 5 (Ozhathil et al. 2018). It seems to have little or no interaction with closely related family members of TRPM4. Even though it is quite new, some studies have already used it as a mean to study the TRPM4 channel and surely more will follow in the next times (Bianchi, Smith, and Abriel 2018, O'Malley et al. 2020).

Recently, the TRPM4 channel has been shown to modulate immune cell function such as that of T cells, dendritic cells (DC), phagocytes and mast cells by means of regulating membrane depolarization and  $\text{Ca}^{2+}$  homeostasis. Indeed, TRPM4 critically determines the driving force for  $\text{Ca}^{2+}$  influx in mast cells and their release of inflammatory mediators (Vennekens et al. 2007). Also cytokine production by T cells is mediated by  $\text{Ca}^{2+}$  oscillations triggered by TRPM4-induced depolarization (Launay, Cheng, et al. 2004). On the other hand, TRPM4 is expressed at different levels in Th cells, being higher in Th2 cells compared with Th1. Inhibition of its expression with siRNA and a DNA construct results in increased  $\text{Ca}^{2+}$  levels and decreased mobility of Th2 cells, and the exact opposite in Th1 (K. S. Weber et al. 2010). The migration of dendritic cells is also very dependent on the  $\text{Ca}^{2+}$  homeostasis provided by TRPM4, without effects on dendritic cell maturation (Barbet et al. 2008). In addition, TRPM4 control of the  $\text{Ca}^{2+}$  influx critical for the proper functioning of phagocytic cells such as monocytes/macrophages and the efficiency of the subsequent response to infection (N. Serafini et al. 2012). Furthermore, it is known that altered ion channel expression is a key feature of MS. It has been reported that in MS a number of ion channels including TRPM4 undergo maldistribution, dysfunction



## CHAPTER 1. INTRODUCTION

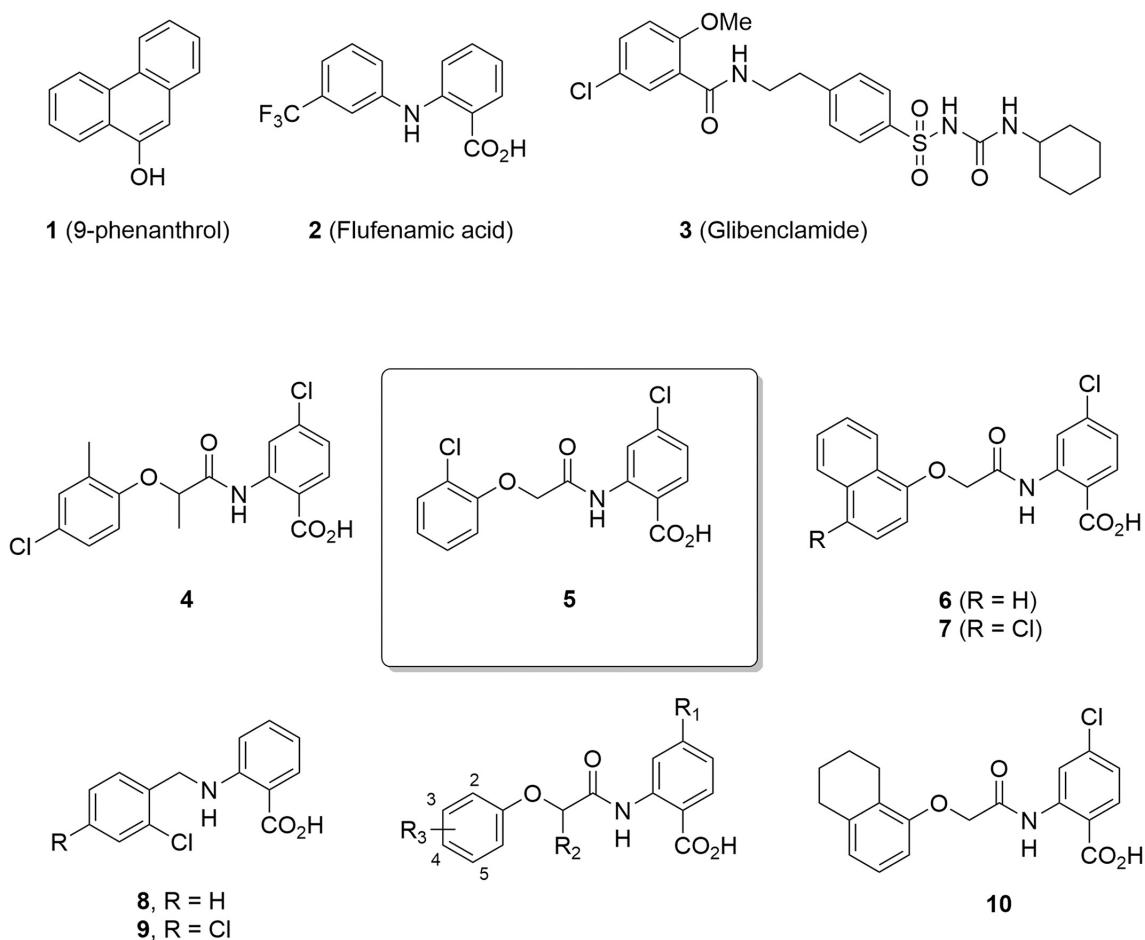


**Figure 1.6: Chemical structures of TRPM4 inhibitors.** In this study compounds 1 (9-Phenanthrol), 3 (Glibenclamide) and 5 (CBA) were used. Figure from Ozhatil et al. 2018.

or pathological activation in a number of different cells (Friese et al. 2007, Craner et al. 2004).

Very important findings for the basis of this thesis were done by Schattling et al. (Schattling et al. 2012) (Figure 1.7). In this paper it was shown that deletion or pharmacological inhibition of TRPM4 with the antidiabetic drug glibenclamide results in reduced neurodegeneration and better clinical disease scores in EAE. Interfering with TRPM4 could therefore, be a neuroprotective treatment strategy. Glibenclamide is a safe and well-known sulfonylurea so it might be used safely in patients with MS to stop disease progression.

A number of recent studies have extended these findings. Recent evidence indicates

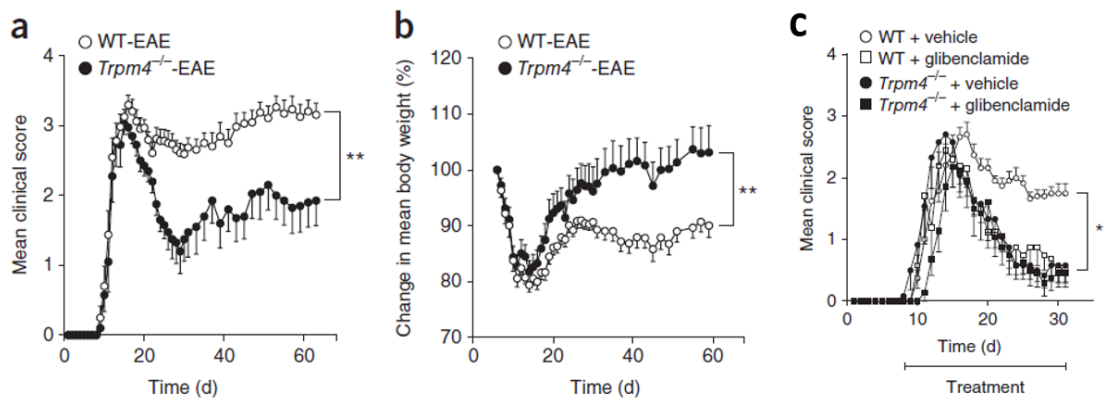


**Figure 1.7: TRPM4 in EAE.** a., b. Disease progression in a mouse model for multiple sclerosis (EAE). TRPM4 knock-out mice partly recover from EAE in comparison to wildtypes. c. Pharmacological inhibition of TRPM4 with Glibenclamide also induces improvement of the clinical score in WT mice. Figure adapted from Schattling et al. 2012.

that SUR1 inhibition results in robust anti-inflammatory effects in CNS injury. In models of cerebral ischemia and spinal cord injury, Glibenclamide inhibition of SUR1 is associated with enhanced microglial phagocytosis and improved neurological function, with these effects attributed to inhibition of microglial SUR1 - Kir6.2 (Caffes et al. 2015). And also in models of subarachnoid hemorrhage and MS, gene suppression or pharmacological inhibition of ATP Binding Cassette Subfamily C Member 8 (*Abcc89*) / SUR1 with glibenclamide significantly ameliorates neuroinflammation and improves neurological function, with these effects being attributed to the inhibition of SUR1 - TRPM4 channels (Kurland et al. 2016). A study from 2015 shows that SUR1 - TRPM4 is upregulated in EAE further suggesting that TRPM4 might represent a target for disease-modifying therapy in MS (Makar et al. 2015). Blocking TRPM4 with 9-Phenanthrol, glibenclamide or CBA reduces cell death in glutamate excitotoxicity assays (Bianchi, Smith, and Abriel 2018, Schattling et al. 2012). A very recent study established that excitotoxicity in the neurons requires the formation of a N-methyl-D-aspartate receptor (NMDAR) / TRPM4 complex. This interaction is mediated in intracellular domains located in the near membrane portions of the receptors. Since TRPM4 has been shown to be absent from the synapse, this complex is formed extrasynaptically to promote death signaling. More exactly, the NMDAR will connect with the SUR1 part of the TRPM4 / SUR1 complex (Yan et al.

## *CHAPTER 1. INTRODUCTION*

2020).

Still the exact role that TRPM4 plays in MS and EAE is not well clarified. In most studies it was assumed, but not definitively demonstrated, that the TRPM4 effects were indeed mediated by neuronal TRPM4. Therefore, my goal was to identify the role of the TRPM4 channel in microglia and to investigate its influence on their fundamental properties.

# Chapter 2

## Materials and Methods

### 2.1 Animals and slice culture

#### 2.1.1 Mice

All mice were housed and bred at the University Medical Center Hamburg-Eppendorf (UKE) animal facility, with a 12-hour light/dark cycle and had water and food *ad libitum*. All the procedures were performed in compliance with the Animal Welfare Law of the Federal Republic of Germany (Tierschutzgesetz der Bundesrepublik Deutschland, TierSchG) and according to the guidelines of the Directive 2010/63/EU. All the experiments, protocols and the study were approved by the local ethics committee (Behörde für Justiz und Verbraucherschutz-Lebensmittelsicherheit und Veterinärwesen Hamburg).

#### 2.1.2 Mouse Genotyping

Tail biopsies were taken from mice at postnatal days 3 – 4 and lysed using 75 µl alkali buffer containing (in mM): 25 NaOH, 0.2 Na<sub>2</sub> - Ethylenediaminetetraacetic acid (EDTA)\*2 H<sub>2</sub>O for 60 min at 95°C, and then neutralized using 75 µl of neutralizing buffer 40 mM Tris - HCl. Polymerase chain reaction (PCR) based genotyping of the Rosa26 locus was performed using the primer combinations:

Trpm4 KO: 5' - GAG TTC CTG TCC TCC TAA AGG - 3' and 5' - CCA AAG CCT AGA CTT AAT TTC C - 3'.

## CHAPTER 2. MATERIALS AND METHODS

Trpm4 WT: 5' - TCC ACC TTT CTT AGT TCA CC - 3' and 5' - GTT TGA TGT CTC CTT CAG TCG - 3'.

tdT: 5' - CTC CAA GGC GTA CGT GAA GC - 3' and 5' - ACT GTT CCA CGA TGG TGT AGT C - 3'.

Cre: 5' - TAA CAT TCT CCC ACC GTC AGT ACG - 3' and 5' - AAA CGT TGA TGC CGG TGA ACG TGC - 3'.

The PCR reaction requires for one sample: 1  $\mu$ l deoxyribonucleic acid (DNA), 10  $\mu$ l Amplitaq (AmpliTaQ Gold® 360 PCR Master Mix), 1  $\mu$ l forward primer (10  $\mu$ M), 1  $\mu$ l reverse primer (10  $\mu$ M), and 7  $\mu$ l H<sub>2</sub>O. For this work, the Cre, tdT and TRPM4 genes were tested.

### 2.1.3 Mouse organotypic slice cultures

Mice carrying a tamoxifen-inducible Cre-recombinase in microglia and the floxed fluorescent marker tdTomato (B6.129; B6.129 - Cx3cr1tm2.1(cre/ERT2)Jung Gt(ROSA26) - Sortm9(CAG-tdTomato)Hze) (JAX 020940; JAX 007909) were crossed with mice heterozygously carrying the Gt(ROSA26)Sortm1(CAG - COP4\*E123T\*H134R, - tdTomato)Gfng (JAX 017455) allele to generate mice expressing tdTomato and Cre in microglia. Organotypic hippocampal slice cultures (OHSC) from sex-matched TRPM4-expressing mice and littermate controls were prepared at postnatal days 4 – 7 according to the description in this protocol (Gee et al. 2017).

Briefly, mice were anesthetized with 80% CO<sub>2</sub> and 20% O<sub>2</sub> and decapitated. Hippocampi were dissected in cold slice culture dissection solution containing (in mM): 248 sucrose, 26 NaHCO<sub>3</sub>, 10 glucose, 4 KCl, 5 MgCl<sub>2</sub>, 1 CaCl<sub>2</sub>, 2 kynurenic acid, and 0.001% phenol red. The pH was 7.4, the osmolarity was 310 – 320 mOsm/kg<sup>-1</sup>, and the solution was saturated with 95% O<sub>2</sub> and 5% CO<sub>2</sub>. The tissue was cut into 410  $\mu$ m thick sections on a tissue chopper and cultured at the medium/air interface on membranes (Millipore PICMORG50) at 37°C in 5% CO<sub>2</sub>.

For the first 48 h of incubation, 1  $\mu$ M (Z) - 4 - hydroxytamoxifen (Sigma H7904) was added to the slice culture medium to induce Cre-dependent recombination. No other antibiotics were added. Two days after the medium was completely replaced by normal medium, followed by a 60 - 70% medium change twice a week, and contained (for 500

## CHAPTER 2. MATERIALS AND METHODS

ml): 394 ml Minimal Essential Medium (Sigma M7278), 100 ml heat inactivated donor horse serum (Sigma H1138), 1 mM L-glutamine (Gibco 25030-024), 0.01  $\text{mg/ml}^{-1}$  insulin (Sigma I6634), 1.45 ml 5 M NaCl (Sigma S5150), 2 mM  $\text{MgSO}_4$  (Fluka 63126), 1.44 mM  $\text{CaCl}_2$  (Fluka 21114), 0.00125% ascorbic acid (Fluka 11140), and 13 mM D-glucose (Fluka 49152). The slices were kept in the incubator under 37°C with 95%  $\text{O}_2$ , 5%  $\text{CO}_2$ . The slice cultures obtained as described were used for experiments between 12 and 20 days *in vitro*.

### 2.2 Two-photon microscopy

The two-photon imaging setup was custom built based on an Olympus BX51WI microscope with a pE - 4000 LED light source for epifluorescence. Power densities of 470 nm and 520 nm light were measured using a 1918 - R powermeter (Newport). The microscope was equipped with a HC Fluotar L 25x 0.95 NA (Leica) objective and image acquisition was controlled by the software Scanimage 2017b (Vidrio) written in MatLab. A Ti:Sapphire laser (Chameleon Ultra, Coherent) controlled by an electro-optic modulator (350 - 80, Conoptics) was used to image microglia by exciting tdTomato at 980 nm. Emitted photons were collected through the objective and oil-immersion condenser (1.4 NA, Olympus) with two pairs of photomultiplier tubes (H7422P - 40, Hamamatsu). 560 DXCR dichroic mirrors and 525/50 and 607/70 emission filters (Chroma) were used to separate green and red fluorescence. Excitation light was blocked by short-pass filters (ET700SP - 2P, Chroma).

Slice cultures were placed in the recording chamber of the microscope and perfused with an oxygenated artificial cerebral spinal fluid (ACSF) containing (in mM): 124 NaCl, 26  $\text{NaHCO}_3$ , 1  $\text{MgSO}_4$ , 4 KCl, 2,4  $\text{CaCl}_2$ , 10 D-glucose, 1  $\text{NaH}_2\text{PO}_4$  (pH 7.4, 308  $\text{mOsm/kg}^{-1}$ ) at  $32 \pm 1$  °C or at  $36 \pm 1$  °C. The ACSF was perfused at a flow rate of 2.2 ml/min. A time of 45 - 60 min was allowed for stabilization of the slice in the chamber before beginning the imaging session.

### 2.2.1 Motility and chemotaxis (laser damage) experiments

At the end of the waiting time, the search for microglia in the slice at a depth of 35 - 50  $\mu\text{m}$  below the surface began. I used Zoom 11 with a z-stack of 3  $\mu\text{m}$  to select microglia with a highly ramified, resting morphology.

For motility experiments Z-stacks of individual microglia (zoom 11, 3  $\mu\text{m}$  step size) were acquired every two minutes. For the experiments using acute block of TRPM4, the respective blocking drug was introduced in the recirculating ACSF solution after 15 min of imaging of the baseline motility, and the recording proceeded over the course of one hour. I performed separate experiments for each one of the TRPM4 blocking drugs. For all of these experiments I always used 9-Phenanthrol (Tocris 4999/50) 30  $\mu\text{M}$ , CBA 5  $\mu\text{M}$  (Tocris 6724/10) and Glibenclamide 20  $\mu\text{M}$  (Tocris 0911/100). I was blinded and administered an aliquot containing either the drug or dimethyl sulfoxide (DMSO).

For the experiments with long-term treatment with the drugs, I applied cell culture medium containing the drug to the slice cultures for 2 days or normal cell culture medium. Again I was always blinded to the condition. Imaging was performed as above except for a total of 10 minutes.

For the chemotaxis experiments, laser tissue damage was performed in a standardized fashion at  $36 \pm 1$   $^{\circ}\text{C}$ . A microglia-free region between three to four microglia was selected. Zoom 6 with a z-stack of 2  $\mu\text{m}$  was used to acquire images of the microglia every two minutes. After 10 minutes I did a laser damage by pointing the IR-laser beam to the center of the field of view and in the middle of the stack for several ms, with a laser wavelength of 840 nm and maximum power. Then I recorded another 20 minutes to see how the microglia reacted to this event. As for the motility experiments I was always blinded to the condition.

Only after all the analysis was completed, I was unblinded.

### 2.2.2 Image analysis

#### 2.2.2.1 Microglial motility

Several analysis steps were incorporated into a semiautomated workflow. Image data were background subtracted (rolling ball radius = 30 pixels) and median filtered (radius

## CHAPTER 2. MATERIALS AND METHODS

= 1 pixel) with ImageJ. In order to correct for small positional shifts that occurred during acquisition, we registered all images from a time-lapse recording to the first image of the series (Efficient subpixel image registration by cross-correlation, version 1.1, MATLAB Central File Exchange). Images were then binarized using Otsu's method (threshold set to 50% calculated value) (Otsu 1979). Based on a maximum projection of both images and binary images, a mask was drawn to define the region considered for motility analysis. Within the masked region, we counted the number of pixels that remained stable, that were lost, and that were gained throughout the time series. The corresponding Matlab software for the analysis of motility then created the Region of interest (ROI) images of the microglia with the extending and retracting areas and based on this the ramification and surveillance indices as well as the surveyed area were calculated (Figure 2.2).

### 2.2.2.2 Microglial response to laser-induced damage (chemotaxis)

I used a semi-automated workflow (Microglia response analyzer, Matlab R2016b, MathWorks®, code available on GitHub) to analyze microglial responses to laser-induced tissue damage. Individual images from a time-lapse series (2D, Number, time step) were median filtered ( $3 \times 3$  kernel size), converted to binary form (Otsu's method), polished using dilation, erosion steps, and filling of holes. A spot (eccentricity  $<0.5$ , size  $>50$  pixel) near the image center was defined as the site at which tissue damage was initiated. The image from the tissue damage time point with detected spot coordinates was presented to the user for visual inspection; the location of the spot was corrected if necessary. For further processing, images prior to the damage time point were averaged (median pixel values) to obtain a background image from which an intensity threshold was calculated (locally adaptive threshold, specificity = 0.5).

All images were then background subtracted and binarized using the intensity threshold. The region around the damage center (spot dilated with a  $9 \times 9$  disc) was masked and objects smaller than 5 pixels were removed. Following polishing using a dilation/erosion ( $5 \times 5$  kernel), step object areas, distances, and positions relative to the damage center sectioned into 36 radial slices were extracted.



## 2.3 Immunohistochemistry

### 2.3.1 Perfusion of animals, treatment of cultures and slice fixation

Mice were transcardially perfused with cold phosphate buffered saline (Phosphate-buffered saline (PBS), pH 7.4), followed by 4% paraformaldehyde in PBS under ketamine (130 mg/kg) and xylazine (10 mg/kg) anesthesia. The brains were extracted and post-fixed for 24 h in 4% paraformaldehyde (PFA) at 4°C. Before slicing, the tissue was changed to 1 x PBS for 20 min, then slices of 40 µm were sectioned using Leica vibratome, collected, and stored in PBS.

Slices were treated with slice culture medium containing Lipopolysaccharide (LPS) with a concentration of 100 ng for 48 h before the fixation.

Organotypic slice cultures were fixed in 4% paraformaldehyde in PBS while being shaken at 100 rev/min for 45 min at room temperature and stored in PBS at 4°C until further use.

### 2.3.2 Staining

Fixed cultures or brain slices from perfused animals were cut out with the membrane and blocked for 2 h at room temperature using 350 µl of goat serum-based blocking solution per well in a 24 - well plate containing (in %): 10 Goat serum (Capricorn), 0.2 Bovine Serum Albumin (Sigma Aldrich A2153 - 10G), and 0.5 TritonX - 100 (Sigma Aldrich T - 9284). After the blocking, the slice cultures were immersed in 350 µl primary antibody in carrier solution per well at 4°C for 48 hours in the dark. Primary antibodies were directed against ionized calcium - binding adapter molecule 1 (IBA1) (rabbit - anti - iba1 WAKO chemicals 019 - 19741 1:1000) and tdTomato (mouse - anti - dsRed Takara 632392 1:1000).

Before application of secondary antibodies, slices were washed three times for 10 minutes with PBS and then incubated with secondary antibodies for 2 h at room temperature. Secondary antibodies were goat anti-rabbit or anti-mouse conjugated with Alexa dye 568 (1:1000), respectively (Life Technologies A11004). Antibodies were prepared in carrier solution containing (in %): 1 Goat serum (Capricorn), 0.2 Bovine Serum Albumin

## CHAPTER 2. MATERIALS AND METHODS

(Sigma Aldrich A2153 - 10G), and 0.5 TritonX - 100 (Sigma Aldrich T - 9284).

Slices were again washed for three times with PBS for 10 minutes, incubated with diamidino - 2 - phenylindole (DAPI) (Molecular Probes, Invitrogen) for 5 min and then mounted. In the end the slices were placed on a microscope slide (Thermo Scientific 9990402). 3 - 6 drops of mounting gel (IMMU - MOUNT form SHANDON) were set around the slices. Finally, the cover glass was placed on top. To prevent the slices from drying, nail polish was put on around the edge of the slide after the mounting gel was firm. Until imaging the slides were stored at 4°C in the dark.

### 2.3.3 Confocal microscopy

Images of the microglia were acquired using Olympus confocal microscopy (Olympus Fluoview FV1000) with the 20 x Oil objective (UPLSAPO 20X NA : 0.85). Images were acquired in one channel (Alexa Fluor 568) in 1024\*1024 pixel, 125 µs/pixel, 0.31 µm/pixel, stack step size Z = 3 µm, frame sequential mode.

For the cell count the images were acquired in two channels (Alexa Fluor 488 and 568) in Z = 1 and otherwise with the same settings and then overlaid.

#### 2.3.3.1 Image analysis of microglial morphology

The images acquired in the confocal microscopy were then exported to Imaris (version 9) software (Bitplane) in order to be analyzed. Using the function Filament tracer, the microglia cell bodies were identified and marked and corrected by hand one by one if needed. The microglial filaments given by the software were also corrected one by one, since the software creates more filaments than the real ones. Then the data were exported to an excel file, which was afterwards imported to Matlab, where a script was used to do the Sholl analysis. This analysis is an approach to evaluate the morphology of microglia designed by the pioneering work of Sholl (Sholl 1953), and consists of a quantitative method to study radial distribution of dendrites in neurons and processes in microglia generated by arborization patterns around the cell body (Milošević and Ristanović 2007). Using this analysis, one can gather information about the number of branches or the order of branching at a certain distance from the cell body. To give such an output the method

## CHAPTER 2. MATERIALS AND METHODS

implies building a series of concentric and equidistant rings around the cell body. It then counts the number of intersections that a cell process has with each individual circle. This is also called the frequency of a process. The method can then define suitable variables such as the ramification index or the maximum number of intersection using the two found parameters: frequency and circle radius (Cătălin et al. 2013). In other words, the greater the number of Sholl intersections, the more ramified the microglia are (Figure 2.1).

Parallel to Filament tracer, the Imaris software tool Spot detection was also used to perform cell count and calculate the ratio of microglia/total cells in Prism (Figure 2.3).

### **2.4 Statistics**

All statistics were performed using Graphpad Prism (version 9). A p-value below 0.05 was considered significant.

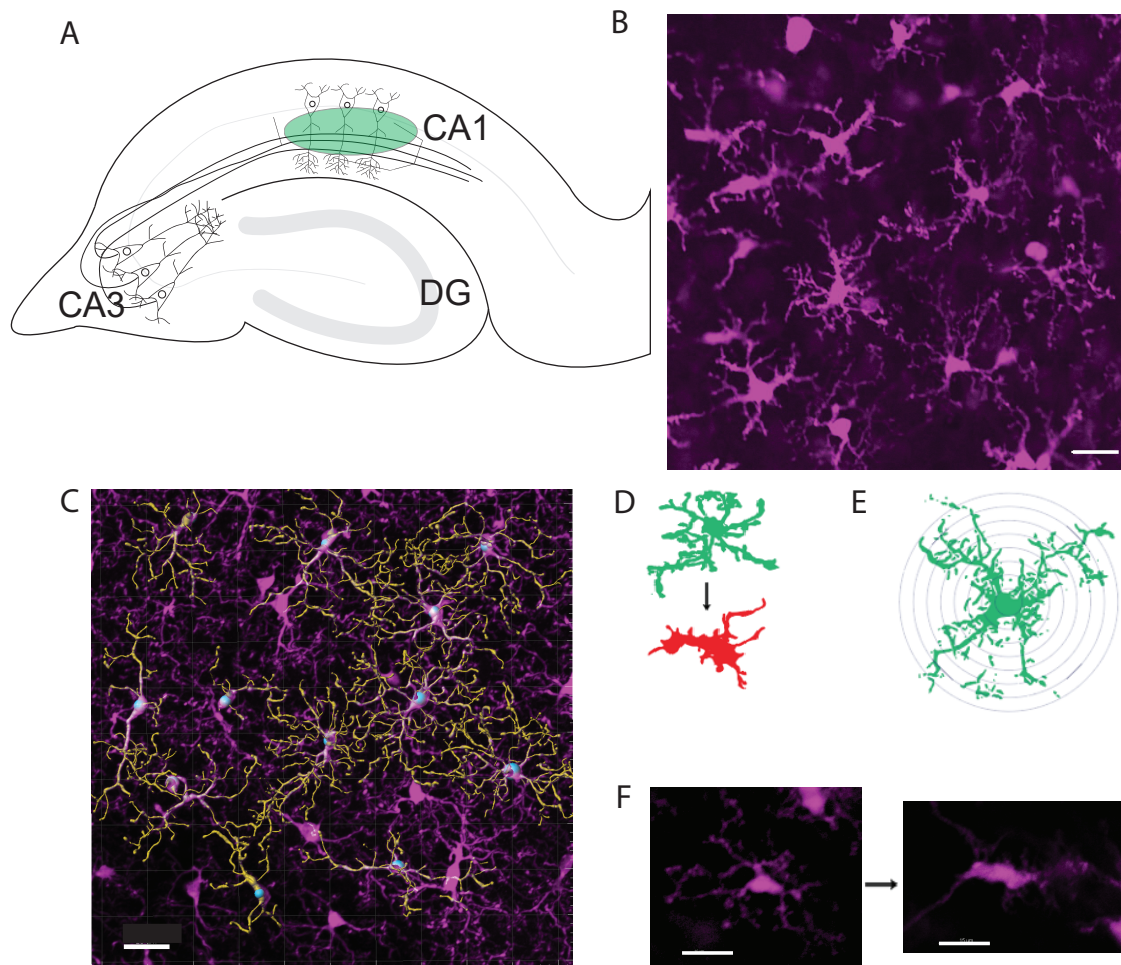


**Figure 2.1: Morphology experiment.** **A** Representation of the mouse hippocampus and in green the targeted area for imaging in this experiment *stratum radiatum* (green ellipse). **B** Staining of microglia with Iba1 in Zoom 3. Scale bar 20  $\mu\text{m}$ . Microglia stained with Iba 1 and representative image of a resting state microglia and its transformation in an activated state one. **C** Overlay of the microglial filaments and somas using the Imaris software and the tool filament tracer. Scale bar 20  $\mu\text{m}$ . **D** Representation of a resting state microglia turning into an activated one upon inflammatory stimulus, with crumbling of processes around the soma. **E** Schematic representation of the Sholl analysis. **F** Stained microglia replicating the process of activation shown schematically in D. Scale bars 15  $\mu\text{m}$ .

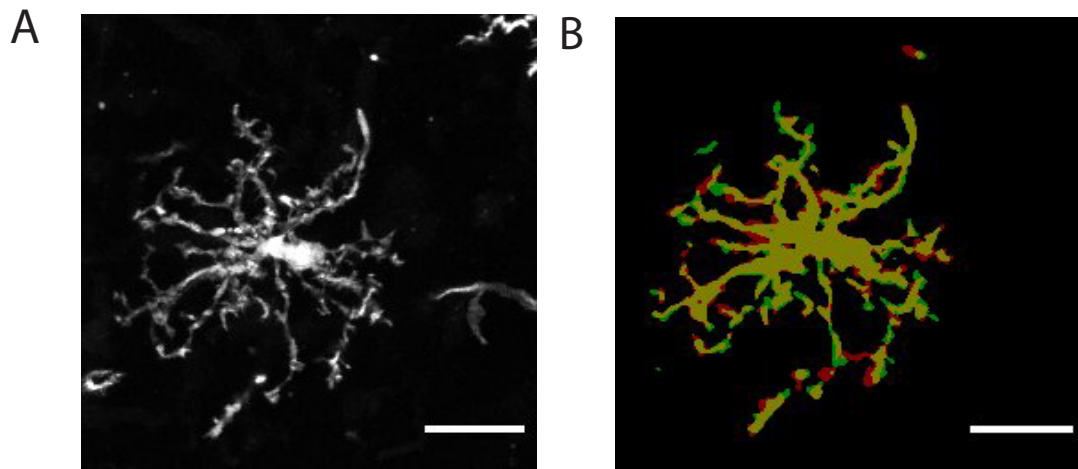


**Figure 2.2: Image analysis of microglial motility.** **A** Maximum projection of the microglia image obtained in the two-photon microscope. Scale bar 20  $\mu\text{m}$ . **B** ROI of the previous image showing in yellow the areas that remain unchanged over time, in red the retracting areas and in green the extending ones. Scale bar 20  $\mu\text{m}$ .

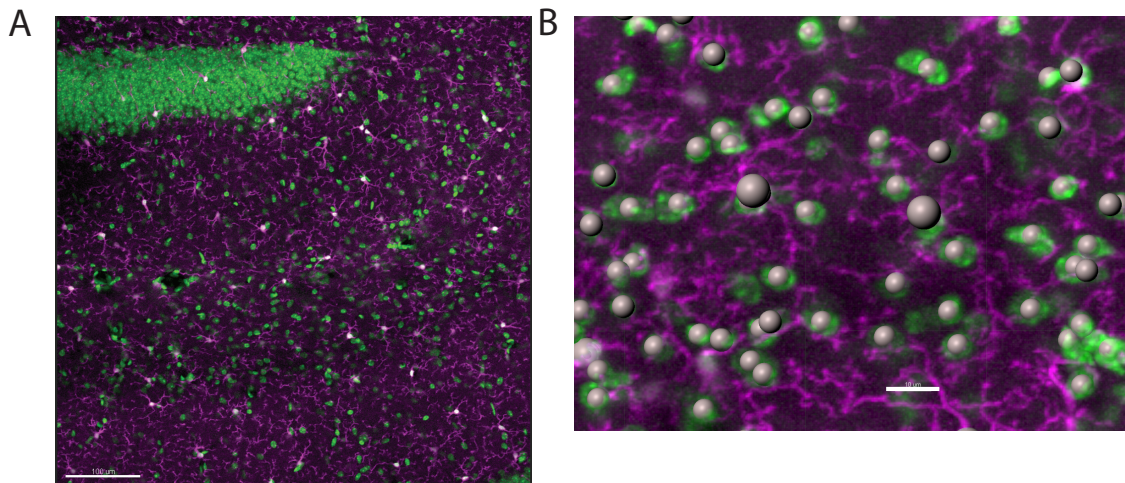


**Figure 2.3: Spot detection.** **A** Overview image of the *stratum radiatum* with Iba1 stained microglia in magenta and DAPI in green. Scale bar 100  $\mu\text{m}$ . **B** Example showing detected microglial nuclei (grey spots) on close-up from A. Scale bar 10  $\mu\text{m}$ .

# Chapter 3

## Results

### 3.1 Microglia motility is not affected by acute block of TRPM4

I examined whether the acute block of TRPM4 with different drugs (9-Phenanthrol, CBA and Glibenclamide) would affect the morphology or movement of microglial processes. My results show that an acute block of TRPM4 using 3 antagonists at 32°C does not have an impact neither on the ramification nor on the surveillance indexes (Figure 3.1). Indeed, the variation of the ramification and surveillance indexes was not significant. More specifically, at 32°C there was a time effect, seen as a slow decrease of the indices but in neither measure was there a significant drug effect. Because TRPM4 is known to be temperature sensitive (Talavera et al. 2005), I repeated the experiment with CBA at 36°C. Here, the time effect was not significant, suggesting the decrease in the ramification and surveillance indices in A and B was due to the lower temperature. Again here, there was no drug effect on microglial motility (Figure 3.1).

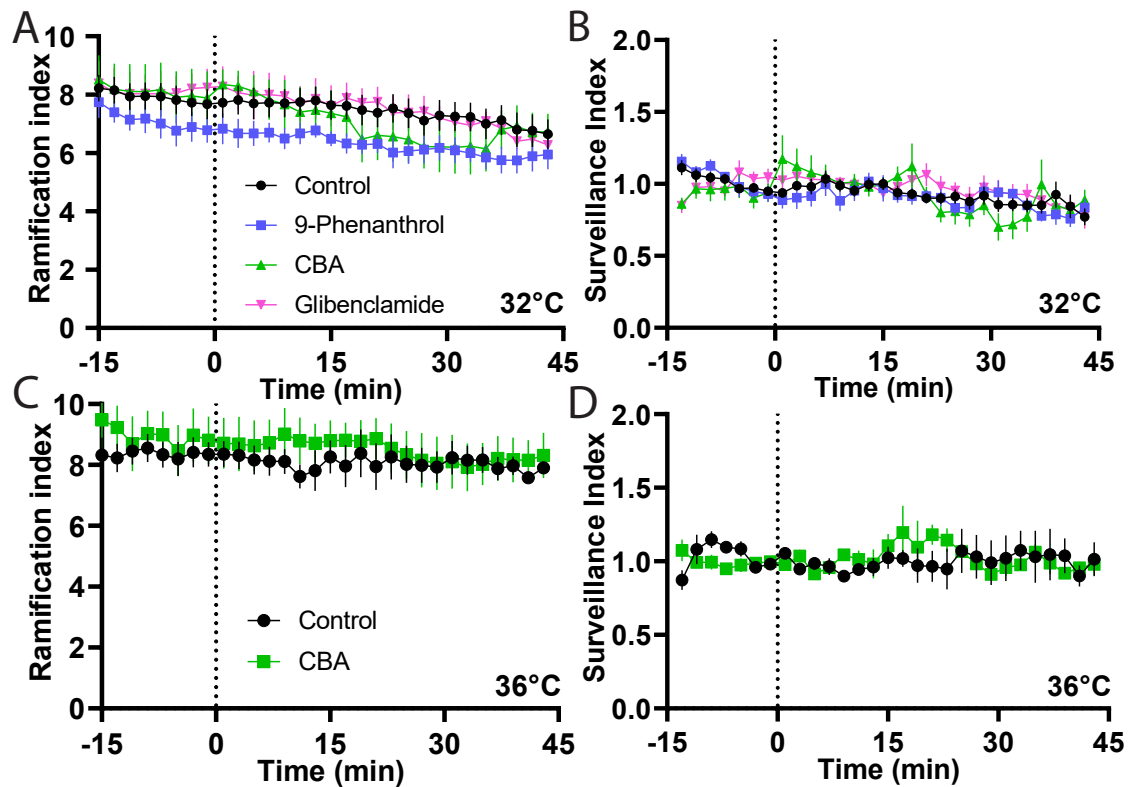


**Figure 3.1: Microglia motility is not affected by acute inhibition of TRPM4.** **A** Ramification index of microglia versus time. The TRPM4 antagonists 9-Phenanthrol (30  $\mu$ M,  $n = 7$ ), CBA (5  $\mu$ M  $n = 7$ ) and Glibenclamide (20  $\mu$ M,  $n = 5$ ) were added at time = 0 indicated by the dotted line at 32°C. Control (DMSO)  $n = 14$  microglia. Two-way ANOVA  $F(3.8, 109.2) = 13.9$   $p < 0.00001$  for time,  $F(3, 29) = 0.7872$   $p = 0.5109$  for drug effect and  $F(87, 840) = 1.009$   $p = 0.4608$  for interaction between time and drug effect. **B** Surveillance index versus time from the same experiments. Two-way ANOVA  $F(7.062, 204.5) = 4.398$   $p < 0.00001$  for time,  $F(3, 29) = 0.3144$   $p = 0.8149$  for drug effect and  $F(84, 811) = 1.196$   $p = 0.1198$  for interaction between time and drug effect. **C** Ramification index of the motility experiment with acute block of TRPM4 using CBA, done at 36°C. Control  $n = 6$  microglia. CBA  $n = 6$ . Two-way ANOVA  $F(4.459, 44.59) = 2.295$   $p = 0.0677$  for time,  $F(1, 10) = 0.2940$   $p = 0.5996$  for drug effect and  $F(29, 290) = 1.026$   $p = 0.4325$  for interaction between time and drug effect. **D** Surveillance index over time in the same experiment. Two-way ANOVA  $F(3.672, 36.72) = 0.6379$   $p = 0.6259$  for time,  $F(1, 10) = 0.02949$   $p = 0.8671$  for drug effect and  $F(28, 280) = 0.9984$   $p = 0.4717$  for interaction between time and drug effect.

## **3.2 Microglia surveillance is not affected by long-term block or KO of TRPM4**

As there was no apparent acute effect of TRPM4 antagonists on microglial motility, in the next experiments I evaluated the ramification index and area surveyed during 10 minutes following chronic blockade (2 days) with CBA. Again I performed the experiments at both 32°C and 36°C. At 32°C there was a clear relationship between surveyed area and ramification index but no effect of CBA (Figure 3.2 A-C). The same was true at 36°C (Figure 3.2 D-F). Very interestingly but not surprisingly, since the temperature sensitivity of the TRPM4 channel has been reported previously, the ramification ( $p < 0,0001$ ) and surveyed areas ( $p = 0,0005$ ) are significantly different in the experiments done on both temperature conditions. (Figure 3.2 G, H). At 32°C, the microglia are less ramified but survey more area, and at 36°C the opposite.

The next step was to check the effect of genetic deletion of TRPM4. The results I obtained showed the KO microglia surveyed more area than the WT ones the more ramified they are (Figure 3.2 I). Furthermore, when I compared the ramification values of the WT microglia with the ones of the KO microglia, a trend has been shown in which the KO microglia tend to be more ramified than the WT ones. This finding was almost significant ( $p = 0,0565$ ), as opposed to the surveyed area, which was not different (Figure 3.2 J, K).



CHAPTER 3. RESULTS

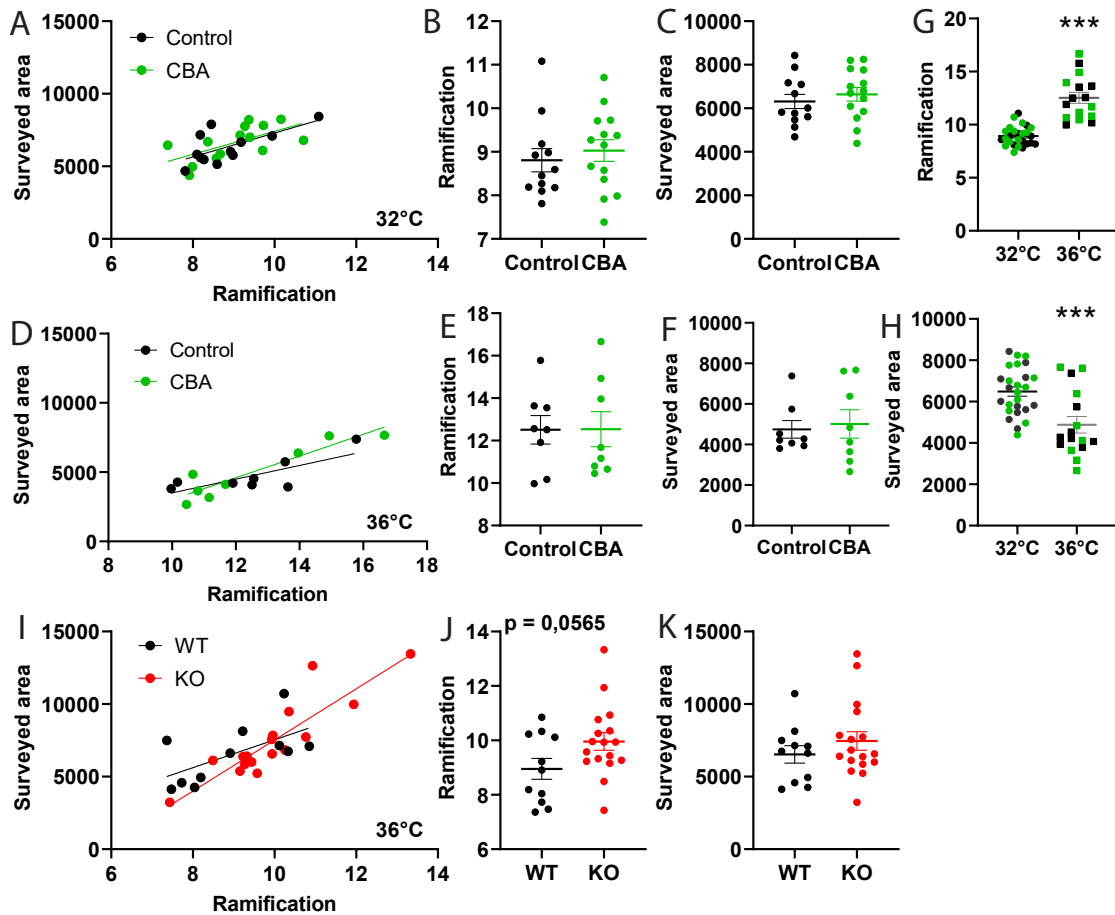


**Figure 3.2: Baseline motility of microglia at 32°C and 36°C.** **A** Surveyed area versus ramification index at 32°C for WT microglia  $n = 12$  ( $Y = 822,5 * X - 931,6$ ;  $R^2 = 0,4438$ ;  $p = 0,0180$ ) and CBA treated  $n = 14$  ( $Y = 791,8 * X - 507,5$ ;  $R^2 = 0,3861$ ;  $p = 0,0177$ ). **B** Ramification index from A. Unpaired t-test  $p = 0,5501$ . **C** Area surveyed in 10 min from A. Unpaired t-test  $p = 0,4789$ . **D** Experiment as in A but at 36°C comparing control microglia  $n = 8$  ( $Y = 495,1 * X - 1450$ ;  $R^2 = 0,5918$ ;  $p = 0,0256$ ) and CBA treated  $n = 8$  ( $Y = 784,3 * X - 4819$ ;  $R^2 = 0,8618$ ;  $p = 0,0009$ ). **E** Ramification index from D. Unpaired t-test  $p = 0,9794$ . **F** Area surveyed in 10 min from D. Unpaired t-test  $p = 0,7473$ . **G** Ramification index of all microglia from A ( $n = 26$ ) and D ( $n = 16$ ). Unpaired t-test  $p < 0,0001$ . **H** Surveyed area of all microglia from A ( $n = 26$ ) and D ( $n = 16$ ). Unpaired t-test  $p = 0,0005$ . **I** Surveyed area versus ramification for WT microglia  $n = 10$  ( $Y = 959,7 * X - 2060$ ;  $R^2 = 0,3824$ ;  $p = 0,0426$ ) and TRPM4-lacking (KO) microglia  $n = 15$  ( $Y = 1761 * X - 10087$ ;  $R^2 = 0,7898$ ;  $p < 0,0001$ ). **J** Ramifications of the WT and KO microglia. Unpaired t-test  $p = 0,0565$ . **K** Surveyed area in 10 min by the WT and KO microglia. Unpaired t-test  $p = 0,3286$ . **B, C, E, F, G, H, I, J, K** Mean  $\pm$  SEM.

### 3.3 LPS-induced inflammation decreases ramification of WT and TRPM4 lacking microglia

From immunostainings I observed that the LPS treatment indeed impacted negatively the ramification of the microglia, both WT and KO (Figure 3.3 A, B). The effect of LPS treatment was also statistically significant in both genotypes compared to the control group. It even seems to be similar independently if it is a WT or a KO microglia, since the difference between both groups with treatment was not significant (Figure 3.3 D). However, the LPS treatment had a much greater impact on the KO microglia, as we see from the graph where the ramification diminished much more with the LPS treatment (Ratio AUC LPS/Control for WT = 0,77 and for KO = 0,54). Additionally and most importantly, the comparison of the untreated slices (Figure 3.3 C) has shown that the KO microglia are more ramified than the WT ones, which stays in tune with the trend observed in the motility experiment. This time, the difference was even statistically significant ( $p = 0,0067$ ). Furthermore, this higher ramification interestingly seems to be in areas of the microglia more distanced to the soma.

### 3.4 KO microglia are also more ramified *ex vivo*

The results I obtained for the stainings *ex vivo* in perfused sliced brains are similar to the ones I obtained for the *in vitro* stainings. This time, I also additionally to these two compared the heterozygous genotype to the KO and WT. Again here, the KO microglia are more ramified than the WT ones (Figure 3.4 A), and also again this difference is more evident in areas more distant to the soma. This difference was almost statistically significant ( $p = 0,0720$ ). The TRPM4 heterozygous microglia are also more slightly more ramified than the WT ones. (Figure 3.4 B) And the morphology of the KO and heterozygous microglia seems to be quite similar. (Figure 3.4 C) The microglia count relative to the total number of cells was obtained using the tool Spot detection from the Imaris software. The ratios tell us that in every genotype the count (Figure 3.4 D) is according to the ratios that are described in the literature (Nimmerjahn, Kirchhoff, and Helmchen 2005).

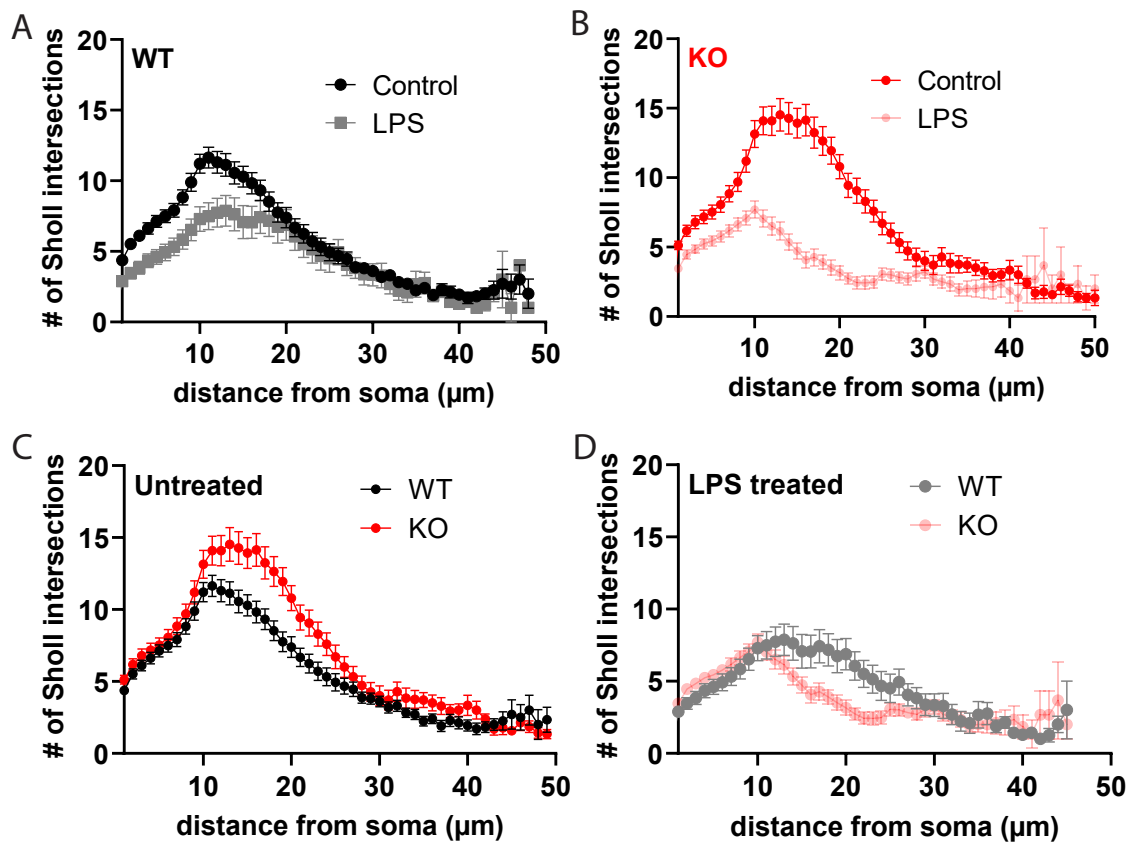


**Figure 3.3: TRPM4 KO microglia are more ramified than WT microglia.** **A** Sholl analysis of microglia from hippocampal slice cultures fixed and stained against Iba1. Control group  $n = 114$  microglia (Area under curve (AUC) =  $264,1 \pm 17,66$ ). Lipopolysaccharide (LPS) treated group 100 ng for 48 h  $n = 105$  (AUC =  $204,2 \pm 21,57$ ). Unpaired t-test for AUC of both groups  $p < 0,0001$  **B** TRPM4 KO microglia. Control group  $n = 54$  microglia (AUC =  $367,7 \pm 25,35$ ). LPS treated group  $n = 187$  (AUC =  $199,9 \pm 14,50$ ). Unpaired t-test for AUC of both groups  $p < 0,0001$  **C** Comparison of the untreated control groups from A, B. KO  $n = 54$  microglia (AUC =  $367,7 \pm 25,35$ ) and WT  $n = 114$  (AUC =  $264,1 \pm 17,66$ ). Unpaired t-test for AUC of both groups  $p = 0,0067$  **D** Comparison of the LPS treated groups from A and B. KO  $n = 187$  microglia (AUC =  $199,9 \pm 14,50$ ) and WT  $n = 105$  (AUC =  $204,2 \pm 21,57$ ). Unpaired t-test for AUC of both groups  $p = 0,6929$ . In brackets: AUC Mean  $\pm$  SEM intersections. $\mu\text{m}$ .

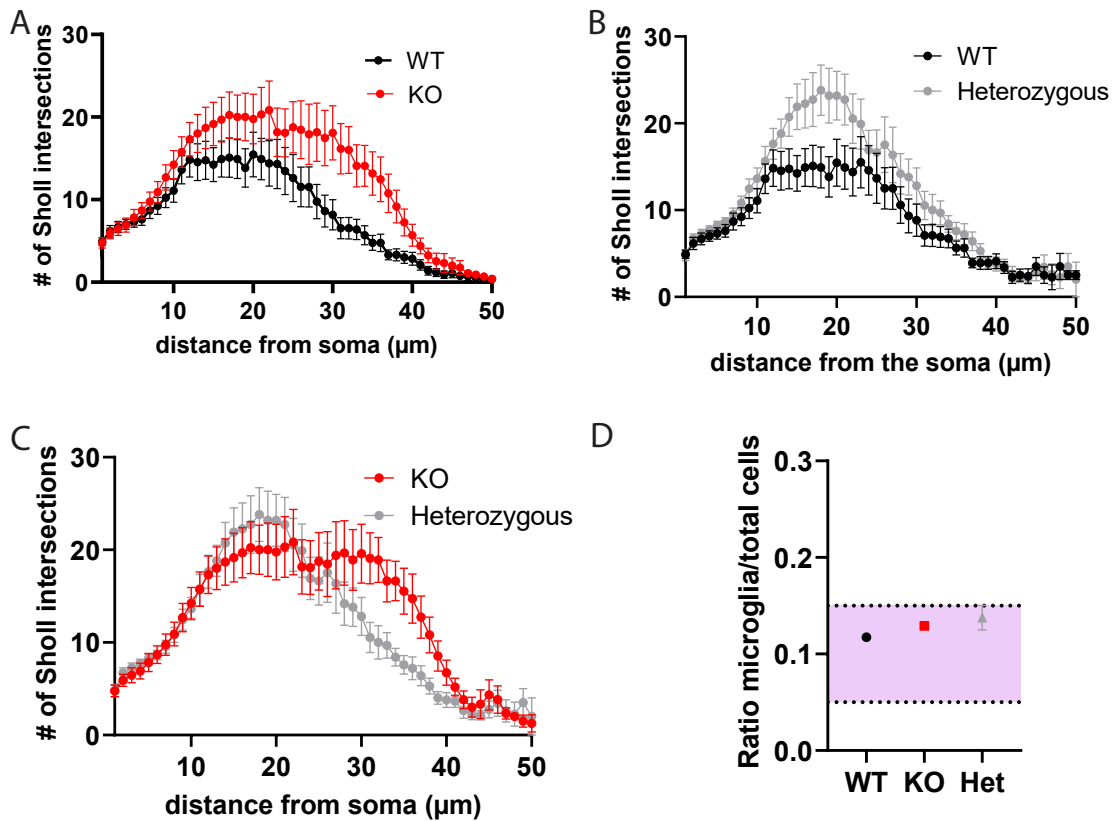


**Figure 3.4: Morphology of TRPM4 KO microglia *ex vivo*.** **A** Sholl analysis of the WT microglia  $n = 13$  microglia (AUC = 402,1  $\pm$  29,40) and TRPM4 KO  $n = 13$  (AUC = 601,7  $\pm$  40,53). Unpaired t-test for AUC of both groups  $p = 0,0720$  **B** WT microglia  $n = 13$  microglia (AUC = 402,1  $\pm$  29,40) and heterozygous  $n = 11$  (AUC = 587,5  $\pm$  29,78). Unpaired t-test for AUC of both groups  $p = 0,0798$  **C** KO microglia  $n = 13$  microglia (AUC = 601,7  $\pm$  40,53) and heterozygous  $n = 11$  (AUC = 587,5  $\pm$  29,78). Unpaired t-test for AUC of both groups  $p = 0,0720$  **D** Ratio of microglia to total cells (DAPI nuclei) in the *stratum radiatum* from the three genotypes Mean  $\pm$  SEM. The dotted lines indicate the normal proportion of microglia (see text). In brackets: AUC Mean  $\pm$  SEM intersections. $\mu\text{m}$

### 3.5 TRPM4 KO microglia respond slower to laser damage than WT ones

The movement of microglial processes is also conditioned by chemical stimuli. Indeed, microglia direct the movement of their processes in a direction when sensing a stimulus in the near environment (Figure 3.5 A). While doing the laser damage experiment, I observed almost always that the microglia processes converged over this time in the direction of the center of the stack. In a few minutes the area is surrounded by microglial pseudopodia (Figure 3.5 C). A small free area indicates the microglia is strongly extending their processes towards the central laser damage. The absence or block of the TRPM4 is also expected to influence the response of the microglia to the laser damage. The diminished calcium influx in the cells would cause a delayed response to an event such as the laser damage.

The application of 9-Phenanthrol has shown that the microglia with this treatment respond much slower than the non-treated ones to the laser damage (Figure 3.5 E). In some experiments the chemotactic response was even completely abolished (Figure 3.5 D). The two-way ANOVA test comparing the free area show a significant difference in the conditions ( $p = 0,0227$ ), as well as a difference over time of the laser damage ( $p < 0,0001$ ) and interaction between time and conditions ( $p < 0,0001$ ).

Afterwards, I performed this experiment in KO microglia and compared the results with a control group of WT microglia. Like I expected, the KO microglia respond much slower than the WT ones to the laser damage (Figure 3.6 A). This variance is significantly different as shown by the two-way ANOVA test, with  $p = 0,0003$  for the different condition and  $p < 0,0001$  for the time and interaction between time and condition. And comparing the different time points using the multiple comparisons test a significance is shown in 4 timepoints after the laser damage.

However, by using the TRPM4 blocking drugs CBA and Glibenclamide (Figure 3.6 B, C), the difference in the response of microglia was not shown to be significant, when comparing WT cultures treated with the drugs for 48h and untreated ones ( $p = 0,8116$  and  $p = 0,1571$  respectively). To note that there is still a time effect in both conditions ( $p < 0,0001$ ), indicating the laser damage has always produced an effect in my experiments.

### *CHAPTER 3. RESULTS*

Lastly, in order to confirm that the TRPM4 blocking drugs I used were exerting their effects directed to this channel, I did this experiment in TRPM4 KO microglia and treated different groups with the three drugs. Not surprisingly, the results have shown that all the KO microglia, treated and untreated, have behaved quite similarly when a laser damaged occurred (Figure 3.6 D), which assures the validity of using these compounds to assess the influence of TRPM4 in the microglia. Again using the two-way ANOVA, a  $p = 0,1178$  shows no significance of the conditions with still an effect of time  $p < 0,0001$ .

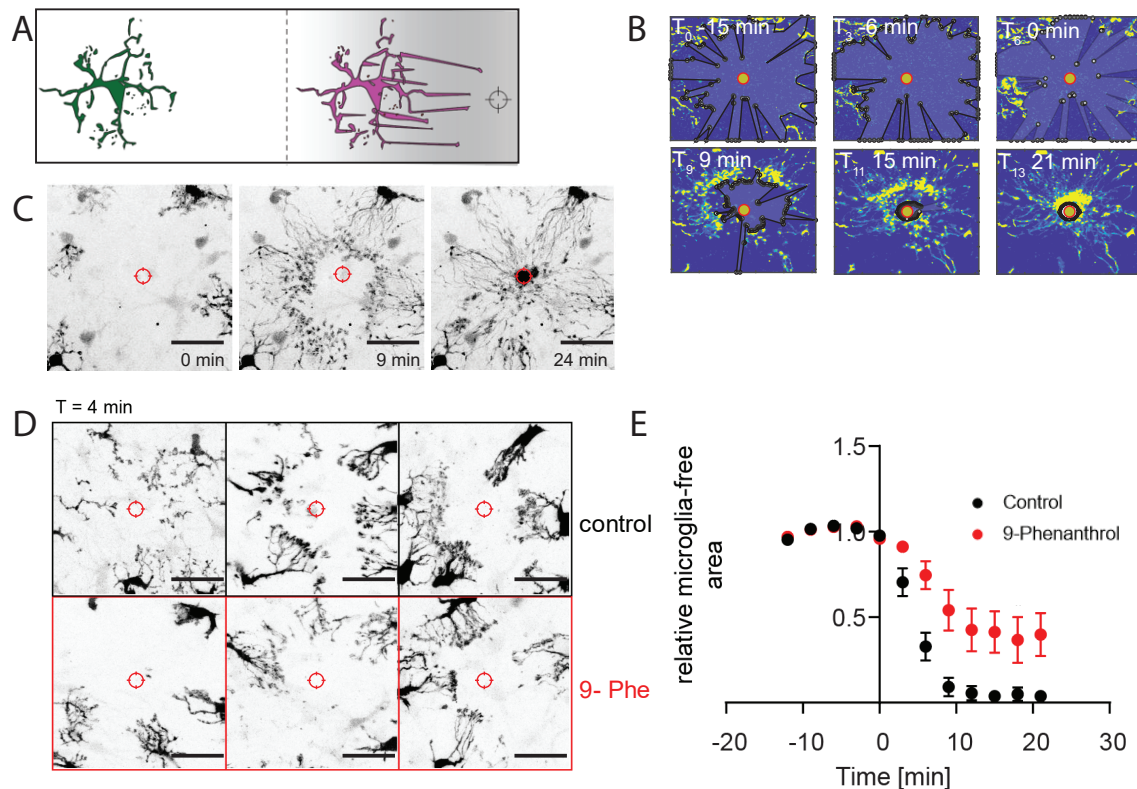


**Figure 3.5: Inhibition of TRPM4 decreases the response of microglia to laser damage.** **A** Schematic representation of the physiological response of microglia and the chemotactic-driven migration of processes in the direction of an aggression in the form of laser damage. **B** Automated MATLAB analysis of chemotaxis quantified as the reduction in microglia-free area around the laser damage (black polygon) at different time points of the experiment. **C** Identification of the microglial processes migration in a two-photon imaging maximum projection in response to a laser damage in the center respectively 0, 9 and 24 minutes after the damage. **D** Examples showing microglial processes (black) at  $t = 4$  minutes after laser damage from 3 control (top) and 3 9-Phenanthrol (bottom) treated slices. **E** Quantification of responses to laser damage from experiments as in D. Control group  $n = 12$  experiments, 9-Phenanthrol  $n = 16$ . Two-way ANOVA  $F(1, 25) = 5,892$   $p = 0,0227$  for drug effect and  $F(1,864, 46,60) = 160,9$   $p < 0,0001$  for time effect and  $F(11, 275) = 3,752$   $p < 0,0001$  for interaction between time and drug effect. Data in this figure from Dr. Laura Laprell. **C, D** Scale bars 50  $\mu\text{m}$ .

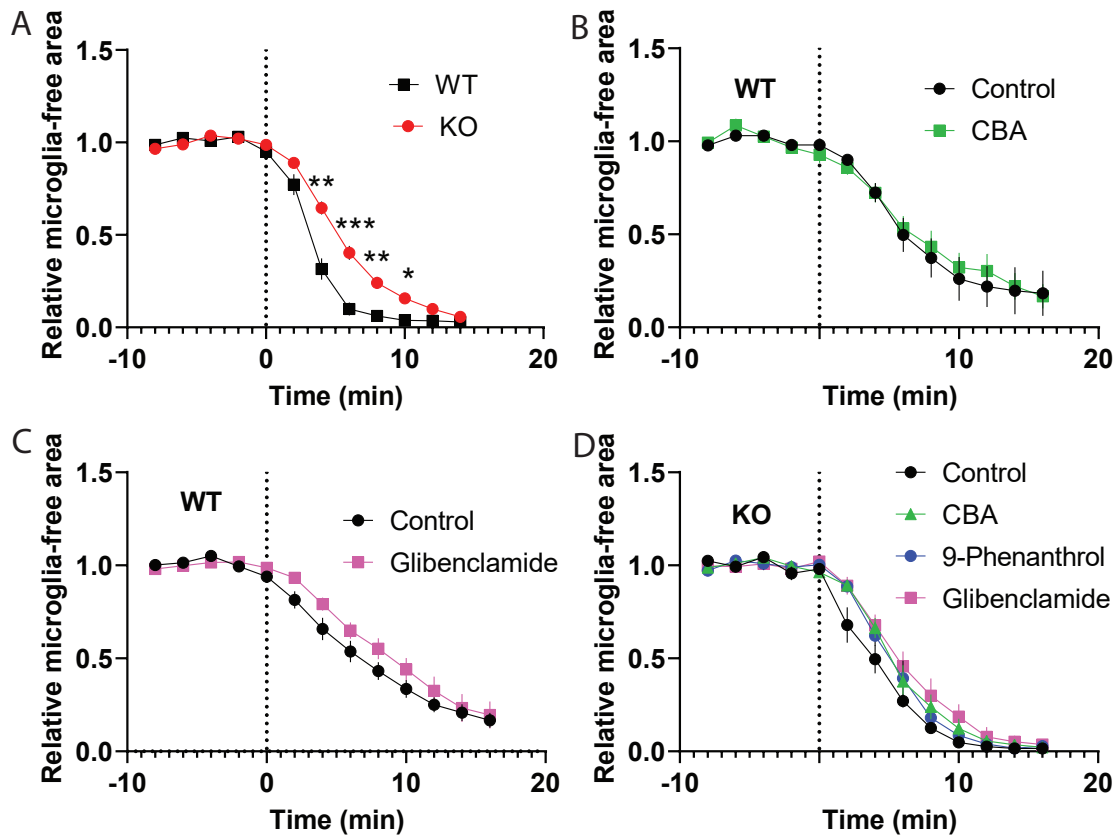


**Figure 3.6: Knock out of TRPM4 decreases the responses of microglia to laser damage.** **A** Microglia-free area before and after laser damage (at  $t = 0$ ). Control  $n = 12$  experiments, KO  $n = 28$ . Two-way ANOVA with  $F(1, 38) = 15,97$   $p = 0,0003$  for drug effect and  $F(3,556, 135,1) = 593,3$   $p < 0,0001$  for time and  $F(11, 418) = 11,77$   $p < 0,0001$  for interaction with time and drug effect. **B** As in A. Control  $n = 8$ , treated with CBA  $n = 9$ . Two-way ANOVA with  $F(1, 15) = 0,05885$   $p = 0,8116$  for drug effect and  $F(1,784, 26,76) = 85,89$   $p < 0,0001$  for time effect and  $F(12, 180) = 0,3094$   $p = 0,9871$  for interaction with time and drug effect. **C** As in A. Control group  $n = 11$ , treated with Glibenclamide  $n = 10$ . Two-way ANOVA with  $F(1, 19) = 2,170$   $p = 0,1571$  for drug effect and  $F(2,815, 53,49) = 165,8$   $p < 0,0001$  for time effect and  $F(12, 228) = 1,339$   $p = 0,1977$  for interaction with time and drug effect. **D** KO microglia in different conditions. Control  $n = 6$ , treated with CBA  $n = 6$ , treated with 9-Phenanthrol  $n = 6$ , treated with Glibenclamide  $n = 5$ . Two-way ANOVA with  $F(3, 19) = 2,230$   $p = 0,1178$  for drug effect and  $F(3,275, 62,22) = 476,2$   $p < 0,0001$  for time effect and  $F(36, 228) = 1,191$   $p = 0,2227$  for interaction with time and drug effect.



# Chapter 4

## Discussion

For the investigation of inflammatory processes in MS, a very good tool is a mouse model for the disease known as EAE. This model is validated since the current available therapies for the disease also seem to be effective in treating EAE (A. P. Robinson et al. 2014). The findings of a 2012 study have shown better clinical disease scores in EAE and reduced neurodegeneration when treating mice with the antidiabetic drug glibenclamide (Schattling et al. 2012). This sulfonylurea can also act as a TRPM4 channel antagonist by blocking the SUR1 receptor, which forms a heteromeric channel with TRPM4 (Woo et al. 2013). The previous study on EAE also reported that with genetic knockout of the TRPM4, mice had better outcomes after the acute phase of EAE supporting the results with pharmacological inhibition ((Figure 1.7). So interfering with TRPM4 is potentially interesting for modulating immune processes leading to neurodegenerative outcomes.

Since most studies on TRPM4 have not fully demonstrated that these effects are mediated by neuronal TRPM4, I set my goal to investigate the role of TRPM4 in microglia, the resident immune cells of the CNS (Perry and Gordon 1988), and whether TRPM4 influences fundamental properties of microglia.

### 4.1 TRPM4 and the motility of microglia

Firstly I aimed to look at the influence of the channel on the motility of microglia. My results for the motility experiments were underwhelming. Blocking TRPM4 with the three different drugs has shown no effects on the motility (Figure 3.1, Figure 3.2 A - F).

Moreover, also the genetic knockout of the channel has produced no significant alterations to the motility parameters (Figure 3.2 I - K).

This property most likely has its basis in actin (Capani, Ellisman, and Martone 2001, Nolte et al. 1996). The movement of microglial processes is what allows them to survey the local environment, a key feature of their immune role of keeping the homeostasis and initiating inflammatory processes (Lampron et al. 2015). So I would expect to see a decrease in the motility indexes and parameters and in the general surveillance of the local environment by the microglia, since the block of TRPM4 has been multiple times presented as a neuroprotective and anti-inflammatory mechanism (Schattling et al. 2012). With this I can state that unfortunately the motility seems to be a poor indicator of microglial activation state and function and not such a useful tool to assess their behaviour as it was theoretically expected.

### 4.2 TRPM4 and the morphology of microglia

An interesting finding appeared though from my motility experiments. The ramifications of the microglia with genetic knockout of the TRPM4 was higher than the WT ones, and this finding was even almost statistically significant (Figure 3.2 J). With this in mind, it seems to make a lot of sense that the experiments I did on morphology of microglia with immunostainings produced results that followed up on this trend.

Indeed, the results of the Sholl analysis (Sholl 1953, Cătălin et al. 2013) showed that the KO microglia are more ramified than the WT ones, both *in vitro* and *ex vivo* (Figure 3.3, Figure 3.4). Interestingly, this difference in the ramification is concentrated on areas of the microglia that are more distal to the soma (Figure 3.3 C). This higher ramification translates into a neuroprotective effect (Zrzavy et al. 2017). Also, my results showed that LPS strongly affects microglial morphology (Abd-El-Basset and Fedoroff 1995) in both WT and KO genotypes (Figure 3.3 A, B), indeed causing microglial activation. I predict that the activation of microglia would contribute to LPS-induced neurotoxicity, as has been reported (Liu et al. 2001). Even though it is known that LPS is rarely present physiologically in the brain *in vivo* since it can not cross the blood-brain-barrier (Banks and S. M. Robinson 2010), it still produces a neuroinflammatory response in microglia

(Wang et al. 2004) and can therefore be used as a useful tool to study their functions.

Based on my results I can state that morphology is a much more powerful tool to assess the microglial function and activated state than motility. Definitely is worthwhile to put effort in further description of the influence of long-term pharmacological block of TRPM4 on microglial morphology by means of immunohistochemistry.

### **4.3 TRPM4 and the laser damage response of microglia**

The chemotatic movement of microglia towards a stimulus is also a powerful predictor of microglia activation state and function (Yao et al. 1990). It was very exciting to obtain a statistically significant result demonstrating that the response of TRPM4-lacking microglia is much slower than the WT ones (Figure 3.6 A). On the other hand, the pharmacological block of the channel did not obtain any remarkable result (Figure 3.6 B, C), except with the antagonist 9-Phenanthrol (Figure 3.5 E).

Indeed, the laser damage experiment with genetic knockout of TRPM4 or its pharmacological block should reveal a decreased response, staying in line with the idea of the neuroprotective role of TRPM4 block (Yin et al. 2020). Behind this idea lies the fact that in 2P microscopy the laser at a high power and intensity can damage the tissue, lysing cells and promoting the release of chemical stimuli, such as purine and pyrimidine analogs, complement factors, cytokines and chemokines, that would lure the microglia into migrating towards that site (Davalos et al. 2005, Honda et al. 2001, Nolte et al. 1996, Zahn et al. 1997, Inoue 2002).

To note that the laser damage experiment is a very good tool to assess microglia because, even though being highly technically demanding to perform, it produces an effect while performing the experiment where one can directly see the processes converge to the central area, and it is a much easier and quicker result to analyze compared to morphology in a immunostaining that needs to go through the Filament tracer tool in Imaris. It is a more direct readout of a function of the microglia.

## 4.4 TRPM4 and temperature

Moreover, in the baseline motility experiment, the parameters I obtained in the same experiment done at different temperatures were different (Figure 3.2 G, H). At a lower temperature, the microglia were less ramified and surveyed more area around them. There was also a clear time effect at the lower temperature, possibly showing an adaptation of the microglia to it. The microglia were at 37°C before starting the experiment, and at 36 °C the controls showed very stable measurements (Figure 3.1 C, D) but at 32 °C there was a steady decrease (Figure 3.1 A, B).

Therefore my results have also corroborated the importance of the tight control of the temperature conditions in experiments focusing on investigating TRPM4 (Talavera et al. 2005) and in a whole number of other members of the TRP family (Nishimoto et al. 2021), since their functions and opening are very temperature sensitive. I consider it valuable that I performed experiments at two different temperature set points and observed this. Temperature can even be used as a tool to investigate TRPM4 in addition to pharmacology and genetic KO.

## 4.5 General considerations and perspectives

Based on all this, it is important to reflect that the genetic knockout of the channel is a much more powerful tool to study the channel, when comparing with the use of different antagonist drugs, since we know genetic knockout is much more specific than the newest antagonists in the market. Nevertheless, pharmacological block of the TRPM4 channel is an easier and more effortless tool to study the channel, compared to genetic knockout. To obtain a transgenic mouse with genetic knockout of the channel involves unfortunately a lot of work including working with mouse lines, organising matings, genotyping and much more. Even though we know that the drugs I used are not completely specific for the TRPM4 channel, my results also show that their use is still valid in spite of this because the KO microglia treated with any of the three drugs did not have an altered response to laser damage (Figure 3.6 D). Still on the topic of pharmacology, it was surprising that the laser damage experiment produced a statistically significant result with the use

## CHAPTER 4. DISCUSSION

of 9-Phenanthrol (Figure 3.5 E) and not with CBA (Figure 3.6 B), which is thought to be the most specific of the three compounds I used (Ozhathil et al. 2018). In further investigation I would consider it to be worthwhile to try out doing these experiments with the newest and more specific TRPM4 antagonists that recently appeared in the market and were proved to block the channel in different extents already in some studies, namely the M4P antibody (Wei et al. 2020), compound 8 and compound 9 (Ozhathil et al. 2018).

When put together, my results show a marked influence of the genetic deletion of the TRPM4 channel in the morphology and chemotaxis of microglia. We know that this can precisely be translated in altered properties of these cells which consequently can have direct implications on the neuroinflammatory response and balance the scale to the neuroprotective side. Without a question this can be of importance for EAE and thus also MS since these cells have an altered phenotype and become activated during the disease (Geladaris, Häusler, and M. S. Weber 2021). It would be very interesting to do some experiments on this matter in mice with EAE and test the different antagonists on them, as well as studying the microglia properties motility, morphology and chemotaxis on slices obtained from these animals. An also interesting topic would be to develop tools that allow for the KO of TRPM4 to be specific in microglia cells.

As a final remark I would like to state the relevance of further studies in this area, both in microglia and TRPM4, for the better understanding of the pathophysiological mechanisms of MS and for trying to establish novel directions for the development of therapeutic options.

# Chapter 5

## Abstract/Zusammenfassung

In a MS mouse model, TRPM4 influences the disease course negatively. Its genetic KO or pharmacological inhibition induces neuroprotective effects. The focus of this study lies on microglial properties and how they are modulated by TRPM4. For this study the TRPM4 antagonists 9-Phenanthrol, Glibenclamide and CBA were used. The assessment of microglia under TRPM4 block by means of 2P microscopy has shown no changes in their motility. However, results of IHC show that their morphology is modulated by the TRPM4, correlating with their transition to an activated, neurodegeneration-promoting state. Their chemotactic response is also hindered by TRPM4 genetic KO. Thus, TRPM4 imposes itself as a key player in modulating microglial dependent inflammatory response and can consequently be a potential target for the control of neurodegenerative processes.

In einem MS Mausmodell hat TRPM4 einen negativen Einfluss auf den Krankheitsverlauf. Pharmakologische Inhibition oder genetischer knock-out führen zu einer Verringerung der Neurodegeneration. Ziel dieser Forschungsarbeit ist es, die Regulationsmechanismen der TRPM4 in Mikroglia zu untersuchen. Hier wurden die TRPM4 Antagonisten 9-Phenanthrol, Glibenclamide und CBA verwendet. Die Ergebnisse der Forschungsarbeit zeigten mittels 2P Mikroskopie keine Veränderung der Mikroglia Motilität. Jedoch wurde deren Morphologie von TRPM4 beeinflusst, korreliert mit ihrem Übergang in einen aktivierten, Neurodegeneration-fördernden State. Zudem verlangsamte TRPM4 KO auch deren Chemotaxis. Demnach spielt TRPM4 eine beachtliche Rolle bei Entzündungsprozessen durch Mikroglia und kann vermutlich Neurodegenerative Prozessen kontrollieren.

# Chapter 6

## List of abbreviations

Abcc89	ATP Binding Cassette Subfamily Member 8
ACSF	Artificial cerebral spinal fluid
ANOVA	Analysis of Variance
ATP	Adenosine Triphosphate
AUC	Area Under Curve
BAFF	B-cell Activating Factor
BBB	Blood Brain Barrier
BTK	Bruton's tyrosine kinase
CBA	4-chloro-2-[[2-(2-chlorophenoxy)acetyl]amino]benzoic acid
CNS	Central Nervous System
CSF-1R	Colony-stimulating factor 1 receptor
CX3CR1	CX3 chemokine receptor 3
DAPI	Diamidino-2-phenylindole
DC	Dendritic cells
DNA	Deoxyribonucleic acid
EAE	Experimental Auto-immuno Encephalomyelitis
EDTA	Ethylenediaminetetraacetic acid
HLA	Human leucocyte antigen
IBA1	Ionized calcium-binding adapter molecule 1
IL	Interleukin

## CHAPTER 6. LIST OF ABBREVIATIONS

KO	Knockout
LPS	Lipopolyssacharide
MOG	Myelin oligodendrocyte glycoprotein
MS	Multiple Sclerosis
NAWM	Normal-appearing White Matter
NMDA	N-methyl-D-aspartate
OHSC	Organotypical Hippocampal slice cultures
P2X4R	Purinergic receptor P2X4
PBS	Phosphate-buffered saline
PCR	Polymerase chain reaction
PFA	Paraformaldehyde
PKC	Protein Kinase C
PIP2	Phosphatidylinositol 4,5-bisphosphate
ROI	Region of interest
ROS	Reactive Oxygen Species
S1P	Sphingosine-1-phosphate
SUR1	Sulfonylurea Receptor 1
tdT	tdTomato
Th	T-helper
TMEM16A	Transmembrane member 16A
TREM2	Triggering receptor expressed in myeloid cells 2
TRP	Transient Receptor Potential
TRPM4	Transient Receptor Potential Melastatin 4
UKE	University Medical Center Hamburg-Eppendorf
WT	Wildtype



# Bibliography

- Abd-El-Basset, E and S Fedoroff (1995). “Effect of bacterial wall lipopolysaccharide (LPS) on morphology, motility, and cytoskeletal organization of microglia in cultures”. In: *Journal of neuroscience research* 41.2, pp. 222–237.
- Aittoniemi, Jussi et al. (2009). “SUR1: a unique ATP-binding cassette protein that functions as an ion channel regulator”. In: *Philosophical Transactions of the Royal Society B: Biological Sciences* 364.1514, pp. 257–267.
- Amor, Sandra et al. (1994). “Identification of epitopes of myelin oligodendrocyte glycoprotein for the induction of experimental allergic encephalomyelitis in SJL and Biozzi AB/H mice.” In: *The Journal of Immunology* 153.10, pp. 4349–4356.
- Ashcroft, Frances M et al. (2005). “ATP-sensitive potassium channelopathies: focus on insulin secretion”. In: *The Journal of clinical investigation* 115.8, pp. 2047–2058.
- Banks, William A and Sandra M Robinson (2010). “Minimal penetration of lipopolysaccharide across the murine blood–brain barrier”. In: *Brain, behavior, and immunity* 24.1, pp. 102–109.
- Barbet, Gaëtan et al. (2008). “The calcium-activated nonselective cation channel TRPM4 is essential for the migration but not the maturation of dendritic cells”. In: *Nature immunology* 9.10, pp. 1148–1156.
- Berghoff, Stefan A et al. (2021). “Microglia facilitate repair of demyelinated lesions via post-squalene sterol synthesis”. In: *Nature neuroscience* 24.1, pp. 47–60.
- Bianchi, Beatrice, Paul A Smith, and Hugues Abriel (2018). “The ion channel TRPM4 in murine experimental autoimmune encephalomyelitis and in a model of glutamate-induced neuronal degeneration”. In: *Molecular brain* 11.1, pp. 1–10.
- Burris, Sarah K et al. (2015). “9-Phenanthrol inhibits recombinant and arterial myocyte TMEM 16 A channels”. In: *British journal of pharmacology* 172.10, pp. 2459–2468.

## BIBLIOGRAPHY

- Caffes, Nicholas et al. (2015). “Glibenclamide for the treatment of ischemic and hemorrhagic stroke”. In: *International journal of molecular sciences* 16.3, pp. 4973–4984.
- Capani, Francisco, Mark H Ellisman, and Maryann E Martone (2001). “Filamentous actin is concentrated in specific subpopulations of neuronal and glial structures in rat central nervous system”. In: *Brain research* 923.1-2, pp. 1–11.
- Cătălin, B et al. (2013). “Microglia branching using a Sholl analysis method”. In: *Curr Health Sci J* 39.Suppl 4, pp. 1–5.
- Compston, Alastair and Alastair Coles (2008). “Multiple Sclerosis”. In: *Lancet* 372, pp. 1502–17.
- Craner, Matthew J et al. (2004). “Molecular changes in neurons in multiple sclerosis: altered axonal expression of Nav1. 2 and Nav1. 6 sodium channels and Na<sup>+</sup>/Ca<sup>2+</sup> exchanger”. In: *Proceedings of the National Academy of Sciences* 101.21, pp. 8168–8173.
- Davalos, Dimitrios et al. (2005). “ATP mediates rapid microglial response to local brain injury in vivo”. In: *Nature neuroscience* 8.6, pp. 752–758.
- Dendrou, Calliope A, Lars Fugger, and Manuel A Friese (2015). “Immunopathology of multiple sclerosis”. In: *Nature Reviews Immunology* 15.9, pp. 545–558.
- Friese, Manuel A et al. (2007). “Acid-sensing ion channel-1 contributes to axonal degeneration in autoimmune inflammation of the central nervous system”. In: *Nature medicine* 13.12, pp. 1483–1489.
- Gee, Christine E et al. (2017). “Preparation of slice cultures from rodent hippocampus”. In: *Cold Spring Harbor Protocols* 2017.2, pdb–prot094888.
- Gees, Maarten, Barbara Colsoul, and Bernd Nilius (2010). “The role of transient receptor potential cation channels in Ca<sup>2+</sup> signaling”. In: *Cold Spring Harbor perspectives in biology* 2.10, a003962.
- Geladaris, Anastasia, Darius Häusler, and Martin S Weber (2021). “Microglia: The Missing Link to Decipher and Therapeutically Control MS Progression?” In: *International Journal of Molecular Sciences* 22.7, p. 3461.
- Ginhoux, Florent et al. (2013). “Origin and differentiation of microglia”. In: *Frontiers in cellular neuroscience* 7, p. 45.

## BIBLIOGRAPHY

- Glatigny, Simon and Estelle Bettelli (2018). “Experimental autoimmune encephalomyelitis (EAE) as animal models of multiple sclerosis (MS)”. In: *Cold Spring Harbor perspectives in medicine* 8.11, a028977.
- Grand, Teddy et al. (2008). “9-phenanthrol inhibits human TRPM4 but not TRPM5 cationic channels”. In: *British journal of pharmacology* 153.8, pp. 1697–1705.
- Henstridge, Christopher M, Makis Tzioras, and Rosa C Paolicelli (2019). “Glial contribution to excitatory and inhibitory synapse loss in neurodegeneration”. In: *Frontiers in cellular neuroscience* 13, p. 63.
- Honda, Shizuyo et al. (2001). “Extracellular ATP or ADP induce chemotaxis of cultured microglia through Gi/o-coupled P2Y receptors”. In: *Journal of Neuroscience* 21.6, pp. 1975–1982.
- Inoue, Kazuhide (2002). “Microglial activation by purines and pyrimidines”. In: *Glia* 40.2, pp. 156–163.
- Jack, Carolyn et al. (2005). “Microglia and multiple sclerosis”. In: *Journal of neuroscience research* 81.3, pp. 363–373.
- Kister, Ilya et al. (2013). “Natural history of multiple sclerosis symptoms”. In: *International journal of MS care* 15.3, pp. 146–156.
- Krumbholz, Markus et al. (2005). “BAFF is produced by astrocytes and up-regulated in multiple sclerosis lesions and primary central nervous system lymphoma”. In: *The Journal of experimental medicine* 201.2, pp. 195–200.
- Kurland, David B et al. (2016). “The Sur1-Trpm4 channel regulates NOS2 transcription in TLR4-activated microglia”. In: *Journal of neuroinflammation* 13.1, pp. 1–23.
- Lampron, Antoine et al. (2015). “Inefficient clearance of myelin debris by microglia impairs remyelinating processes”. In: *Journal of Experimental Medicine* 212.4, pp. 481–495.
- Launay, Pierre, Henrique Cheng, et al. (2004). “TRPM4 regulates calcium oscillations after T cell activation”. In: *Science* 306.5700, pp. 1374–1377.
- Launay, Pierre, Andrea Fleig, et al. (2002). “TRPM4 is a Ca<sup>2+</sup>-activated nonselective cation channel mediating cell membrane depolarization”. In: *Cell* 109.3, pp. 397–407.
- Liman, Emily R (2014). “Trpm5”. In: *Mammalian Transient Receptor Potential (TRP) Cation Channels*, pp. 489–502.

## BIBLIOGRAPHY

- Liu, Bin et al. (2001). “Molecular consequences of activated microglia in the brain: over-activation induces apoptosis”. In: *Journal of neurochemistry* 77.1, pp. 182–189.
- Lloyd, Amy F et al. (2019). “Central nervous system regeneration is driven by microglia necroptosis and repopulation”. In: *Nature neuroscience* 22.7, pp. 1046–1052.
- Lublin, Fred D et al. (2014). “Defining the clinical course of multiple sclerosis: the 2013 revisions”. In: *Neurology* 83.3, pp. 278–286.
- Lucchinetti, Claudia F et al. (2011). “Inflammatory cortical demyelination in early multiple sclerosis”. In: *New England Journal of Medicine* 365.23, pp. 2188–2197.
- Magliozzi, Roberta et al. (2007). “Meningeal B-cell follicles in secondary progressive multiple sclerosis associate with early onset of disease and severe cortical pathology”. In: *Brain* 130.4, pp. 1089–1104.
- Makar, Tapas K et al. (2015). “Silencing of *Abcc8* or inhibition of newly upregulated *Sur1-Trpm4* reduce inflammation and disease progression in experimental autoimmune encephalomyelitis”. In: *Journal of neuroinflammation* 12.1, pp. 1–13.
- McDonald, Ian and Alastair Compston (2006). “The symptoms and signs of multiple sclerosis”. In: *McAlpine’s multiple sclerosis* 4, pp. 321–322.
- Milošević, Nebojša T and Dušan Ristanović (2007). “The Sholl analysis of neuronal cell images: semi-log or log–log method?” In: *Journal of theoretical biology* 245.1, pp. 130–140.
- Moriconi, Emil J, Friedrich T Wallenberger, and William F O’Connor (1959). “A new synthesis of 9-phenanthrol; absorption spectra of the quinhydrone-type molecular compound between 9-phenanthrol and phenanthrenequinone”. In: *The Journal of Organic Chemistry* 24.1, pp. 86–90.
- Nilius, Bernd et al. (2005). “Regulation of the Ca<sup>2+</sup> sensitivity of the nonselective cation channel TRPM4”. In: *Journal of biological chemistry* 280.8, pp. 6423–6433.
- Nimmerjahn, Axel, Frank Kirchhoff, and Fritjof Helmchen (2005). “Resting microglial cells are highly dynamic surveillants of brain parenchyma in vivo”. In: *Science* 308.5726, pp. 1314–1318.
- Nishimoto, Rei et al. (2021). “Thermosensitive TRPV4 channels mediate temperature-dependent microglia movement”. In: *Proceedings of the National Academy of Sciences* 118.17.

## BIBLIOGRAPHY

- Nolte, C et al. (1996). “Complement 5a controls motility of murine microglial cells in vitro via activation of an inhibitory G-protein and the rearrangement of the actin cytoskeleton”. In: *Neuroscience* 73.4, pp. 1091–1107.
- O’Malley, John J et al. (2020). “TRPM4 conductances in thalamic reticular nucleus neurons generate persistent firing during slow oscillations”. In: *Journal of Neuroscience* 40.25, pp. 4813–4823.
- O’Loughlin, Elaine et al. (2018). “Microglial phenotypes and functions in multiple sclerosis”. In: *Cold Spring Harbor perspectives in medicine* 8.2, a028993.
- Otsu, Nobuyuki (1979). “A threshold selection method from gray-level histograms”. In: *IEEE transactions on systems, man, and cybernetics* 9.1, pp. 62–66.
- Ozhathil, Lijo Cherian et al. (2018). “Identification of potent and selective small molecule inhibitors of the cation channel TRPM4”. In: *British journal of pharmacology* 175.12, pp. 2504–2519.
- Perry, V Hugh and Siamon Gordon (1988). “Macrophages and microglia in the nervous system”. In: *Trends in neurosciences* 11.6, pp. 273–277.
- Poel, Marlijn van der et al. (2019). “Transcriptional profiling of human microglia reveals grey–white matter heterogeneity and multiple sclerosis-associated changes”. In: *Nature communications* 10.1, pp. 1–13.
- Raivich, Gennadij et al. (1999). “Neuroglial activation repertoire in the injured brain: graded response, molecular mechanisms and cues to physiological function”. In: *Brain research reviews* 30.1, pp. 77–105.
- Robinson, Andrew P et al. (2014). “The experimental autoimmune encephalomyelitis (EAE) model of MS: utility for understanding disease pathophysiology and treatment”. In: *Handbook of clinical neurology* 122, pp. 173–189.
- Rossum, Denise van and Uwe-Karsten Hanisch (2004). “Microglia”. In: *Metabolic brain disease* 19.3, pp. 393–411.
- Schattling, Benjamin et al. (2012). “TRPM4 cation channel mediates axonal and neuronal degeneration in experimental autoimmune encephalomyelitis and multiple sclerosis”. In: *Nature medicine* 18.12, pp. 1805–1811.

## BIBLIOGRAPHY

- Serafini, Nicolas et al. (2012). “The TRPM4 channel controls monocyte and macrophage, but not neutrophil, function for survival in sepsis”. In: *The Journal of Immunology* 189.7, pp. 3689–3699.
- Shahi, Shailesh K et al. (2019). “Scoring disease in an animal model of multiple sclerosis using a novel infrared-based automated activity-monitoring system”. In: *Scientific reports* 9.1, pp. 1–11.
- Sholl, Donald A (1953). “Dendritic organization in the neurons of the visual and motor cortices of the cat”. In: *Journal of anatomy* 87.Pt 4, p. 387.
- Simard, J Marc et al. (2012). “Sulfonylurea receptor 1 in central nervous system injury: a focused review”. In: *Journal of Cerebral Blood Flow & Metabolism* 32.9, pp. 1699–1717.
- Talavera, Karel et al. (2005). “Heat activation of TRPM5 underlies thermal sensitivity of sweet taste”. In: *Nature* 438.7070, pp. 1022–1025.
- Trepel, Martin (2017). *Neuroanatomie: Struktur und Funktion*. Fischer Gustav Verlag GmbH & Company KG.
- Vennekens, Rudi et al. (2007). “Increased IgE-dependent mast cell activation and anaphylactic responses in mice lacking the calcium-activated nonselective cation channel TRPM4”. In: *Nature immunology* 8.3, pp. 312–320.
- Wang, Tongguang et al. (2004). “Role of reactive oxygen species in LPS-induced production of prostaglandin E2 in microglia”. In: *Journal of neurochemistry* 88.4, pp. 939–947.
- Weber, K Scott et al. (2010). “Trpm4 differentially regulates Th1 and Th2 function by altering calcium signaling and NFAT localization”. In: *The Journal of Immunology* 185.5, pp. 2836–2846.
- Wei, Shunhui et al. (2020). “Comparison of Anti-oncotic Effect of TRPM4 Blocking Antibody in Neuron, Astrocyte and Vascular Endothelial Cell Under Hypoxia”. In: *Frontiers in Cell and Developmental Biology* 8, p. 1175.
- Woo, Seung Kyoon et al. (2013). “The sulfonylurea receptor 1 (Sur1)-transient receptor potential melastatin 4 (Trpm4) channel”. In: *Journal of Biological Chemistry* 288.5, pp. 3655–3667.

## BIBLIOGRAPHY

- Yan, Jing et al. (2020). “Coupling of NMDA receptors and TRPM4 guides discovery of unconventional neuroprotectants”. In: *Science* 370.6513.
- Yao, J et al. (1990). “Chemotaxis by a CNS macrophage, the microglia”. In: *Journal of neuroscience research* 27.1, pp. 36–42.
- Yin, Ping et al. (2020). “Maresin1 Decreased Microglial Chemotaxis and Ameliorated Inflammation Induced by Amyloid- $\beta$  42 in Neuron-Microglia Co-Culture Models”. In: *Journal of Alzheimer’s Disease* 73.2, pp. 503–515.
- Zahn, Joachim von et al. (1997). “Microglial phagocytosis is modulated by pro-and anti-inflammatory cytokines”. In: *Neuroreport* 8.18, pp. 3851–3856.
- Zhang, Yifeng et al. (2003). “Coding of sweet, bitter, and umami tastes: different receptor cells sharing similar signaling pathways”. In: *Cell* 112.3, pp. 293–301.
- Zhang, Zheng et al. (2005). “Phosphatidylinositol 4, 5-bisphosphate rescues TRPM4 channels from desensitization”. In: *Journal of Biological Chemistry* 280.47, pp. 39185–39192.
- Zrzavy, Tobias et al. (2017). “Loss of ‘homeostatic’ microglia and patterns of their activation in active multiple sclerosis”. In: *Brain* 140.7, pp. 1900–1913.

# Chapter 7

## Acknowledgements

My thesis could not have possibly been accomplished without the help and support of many people. Here I want to take the opportunity to mention them and thank them from the heart.

First of all, thank you to my supervisors Dr. Laura Laprell and Dr. Christine Gee. You both took me into this project and into the lab, always giving me great ideas and teaching me so much. Thank you for being such attentive and caring supervisors. Laura accompanied me through all my different experiments, integrated me in the microglia group daily life and always saw something in me and believed in me. I have such great admiration for her being an amazing and genius scientist. And Chris with her deepest knowledge of the field always had the best advice and remarks, while also being available at all times and guiding me scientifically through the whole process. Also thank you to my institute director Prof. Thomas Oertner for giving me the opportunity to work in his lab and for having the great technical expertise that I so often needed. I would also like to thank Dr. Christian Schulze for collaborating with Dr. Laura Laprell for the development of the MatLab softwares I used throughout this study. A very big thank you to my members of the microglia group Marie and Della, who also became my friends. Without you none of this would have been possible because my belief in myself came from you believing more in me. You both have always had patience with me and taught me everything in the lab since the basics, allowing me to also do science. With you both I also had the funniest moments, either in the lab's working benches or on our walks to the Isemarkt. Besides I want to thank all my lab members from the Oertner group



## CHAPTER 7. ACKNOWLEDGEMENTS

because you all in one way or the other contributed not only to this thesis but also for the great work environment I experienced daily and made me glad to come everyday to work. I always felt surrounded by geniuses and you all are very hardworking and exemplary neuroscientists.

Besides everyone in the lab I would also like to thank my family, mãe, pai, irmã, avó e avô, for always being supportive of my decisions, caring about me and being very loving and encouraging. I missed you so much while doing this project. Thank you for regularly sending me portuguese food. Also to my friends outside the lab who have enormously carried me through the time I spent doing this project and with whom at the same time I lived some of the best moments ever and hope to keep living. You all know you are and Mikel, Myriam, Julika and Ana made me smile the most. Also Jinny, Sophia and Lotti, who are crazy enough to live with me, respect.

I cannot put into words how grateful I am for all this and seeing this thesis all put together is pure joy. I have learned so much about neuroscience and medicine and acquired so many skills. So lucky I was all my life for all the great opportunities that the universe made appear in my life, for being able to take them and accomplish something. Even though I recognize and merit myself for working hard and pushing myself I cannot ignore how privileged I am in every possible sense of the word for all this and, as a final remark, I just wish someday the world will become a place where all individuals can freely and fearlessly be who they are, be kind to each other and have all the opportunities they deserve.

# Chapter 8

## Curriculum Vitae

### Personal Information:

Name Ana Margarida Cavaco Antunes  
Born 08.11.1996 in Lisbon, Portugal

### Education:

Since 07/2020 Medical doctoral thesis at the Oertner Group, Zentrum für Molekuläre Neurobiologie Hamburg  
09/2019 - 06/2020 Final internship, Universitätsklinikum Hamburg-Eppendorf  
09/2018 - 07/2019 Exchange studies, Universitätsklinikum Hamburg-Eppendorf  
09/2014 - 06/2020 Medicine, NOVA Medical School Lisbon (grade 1.7)  
06/2014 Abitur (grade 1.0)

### Grants:

Since 09/2020 Graduiertenkolleg des Hamburg School for Immunity and Infection, SFB 1328 IRTG Adenine nucleotides in immunity and inflammation  
Since 09/2020 medMS Doktorandenprogramm, Gemeinnützige Hertie Stiftung  
09/2019 - 06/2020 Grant agreement Erasmus+ EU Internships  
09/2018 - 07/2019 Grant agreement Erasmus+ EU Studies

# Chapter 9

## Eidesstattliche Versicherung

Ich versichere ausdrücklich, dass ich die Arbeit selbständig und ohne fremde Hilfe verfasst, andere als die von mir angegebenen Quellen und Hilfsmittel nicht benutzt und die aus den benutzten Werken wörtlich oder inhaltlich entnommenen Stellen einzeln nach Ausgabe (Auflage und Jahr des Erscheinens), Band und Seite des benutzten Werkes kenntlich gemacht habe. Ferner versichere ich, dass ich die Dissertation bisher nicht einem Fachvertreter an einer anderen Hochschule zur Überprüfung vorgelegt oder mich anderweitig um Zulassung zur Promotion beworben habe. Ich erkläre mich einverstanden, dass meine Dissertation vom Dekanat der Medizinischen Fakultät mit einer gängigen Software zur Erkennung von Plagiaten überprüft werden kann.

Unterschrift: .....